7400R-Revision 2

A reassessment of the amphibole-plagioclase NaSi–CaAl exchange thermometer with applications to igneous and high-grade metamorphic rocks

José Francisco Molina[1*], Aitor Cambeses[1,2], Juan Antonio Moreno[1,3], Irene Morales[1], Pilar Montero[1], Fernando Bea[1]

1: Department of Mineralogy and Petrology, Campus Fuentenueva, University of Granada, Granada, Spain.

2: Ruhr-Universität Bochum, Fakultät für Geowissenschaften, Institut für Geologie, Mineralogie and Geophysik, Bochum, Germany.

3: Centro de Investigaciones en Ciencias de la Tierra, Consejo Nacional de Investigaciones Científicas y Técnicas. Facultad de Ciencias Exactas, Físicas y Naturales, Universidad Nacional de Córdoba, Córdoba, Argentina.

*Corresponding author: jfmolina@ugr.es

E-mails

J.F. Molina: jfmolina@ugr.es

A. Cambeses: aitorc@ugr.es

J.A. Moreno: jmoreno_2@ugr.es

I. Morales: iremoral@ugr.es

P. Montero: pmontero@ugr.es

F. Bea: fbea@ugr.es

DOI: https://doi.org/10.2138/am-2021-7400. http://www.minsocam.org/

Abstract

The amphibole-plagioclase NaSi–CaAl exchange thermometer by Holland and Blundy (1994 — expression B) has been extensively applied to calcic amphibole-bearing assemblages from metamorphic and igneous rocks, whereas the more recent calibrations of the amphibole-only thermometer by Ridolfi and Renzulli (2012 — expression 2) and Putirka (2016 — expressions 5 and 6) are employed for determining amphibole-saturation temperatures in hydrous magmas. However, a test of these expressions performed on experimental data compiled from the literature reveals significant inaccuracies, tending expression B to underestimate temperatures in high-Mg amphibole, and the amphibole-only expressions to overestimate temperatures in amphibole with either low Mg or high Al^{VI} occupancies. Amphibole Na^{M4} and Fe^{3+} occupancies can also affect significantly the accuracy of expression B.

In this work, we present *three new accurate calibrations* (expressions A1, A2 and B2) of the *amphibole-plagioclase NaSi–CaAl exchange thermometer* calculated by robust regression methods based on multiple maximum-likelihood estimators (MM-estimators; Yohai, 1987), considering various calibration and test data subsets to evaluate the robustness of the derived parameters in the thermodynamic models, and the accuracy and precision of the expressions. Non-ideality in plagioclase was corrected using the ternary feldspar solution model of Elkins and Grove (1990) in expressions A1 and A2, whereas the simplified version of the Darken's Quadratic Formalism (DQF) approach of Holland and Powell (1992) was used in expression B2. The formulation of the multisite macroscopic solution model of Powell and Holland (1993) was used for deriving the mixing parameters of amphibole in the three calibrations. Expression B2 is strictly pressure-independent, while the two others show a negligible dependence on pressure for plagioclase with low orthoclase component (< 11 mol%). The three calibrations yield an overall precision close to those reported for the tested amphibole-based thermometers, but are significantly more accurate, *a requisite for an unambiguous interpretation of precision*.

The new expressions can be used in a wide range of igneous and high-grade metamorphic rocks that bear *subcalcic to calcic amphibole and oligoclase or more calcic plagioclase*. However, they must be applied only to amphibole-plagioclase pairs whose compositions lie in the optimal region of use prescribed in the work.

Keywords: thermometry, calcic amphibole, plagioclase, mixing properties, high-grade metamorphic rocks, metaluminous igneous rocks.

This is the peer-reviewed, final accepted version for American Mineralogist, published by the Mineralogical Society of America.
The published version is subject to change. Cite as Authors (Year) Title. American Mineralogist, in press.
DOI: https://doi.org/10.2138/am-2021-7400. http://www.minsocam.org/

Introduction

Calcic amphibole is an important constituent of basic to acid metaluminous igneous rocks and their metamorphic derivatives (e.g., Robinson et al., 1982; Wones and Gilbert, 1982; Martin, 2007; Schumacher, 2007). Many studies have been devoted to determine its P-T-X relationships in both synthetic and natural assemblages (e.g., Czamanske and Wones, 1973; Laird and Albee, 1981; Thompson et al., 1982; Apted and Liou, 1983; Poli, 1993; Spear, 1993; Molina and Poli, 1998, 2000; García-Casco et al., 2008; Molina et al., 2009; Bucher and Grapes, 2011; Castro, 2013; Werts et al., 2020). These studies have provided a basis for the calibration of numerous thermometers and barometers that make it possible to determine the P-T conditions of crystallization/re-equilibration of amphibole-bearing assemblages. Some widely used calibrations are based on *exchange equilibria* between amphibole and garnet (e.g., Graham and Powell, 1984; Dale et al., 2000; Ravna, 2000), and amphibole and plagioclase (Spear, 1980; Fershtater, 1990; Holland and Blundy, 1994; Molina et al., 2015), and on *net-transfer equilibria* involving amphibole-plagioclase-quartz (Spear, 1981; Blundy and Holland, 1990; Holland and Blundy, 1994; Bhadra and Bhattacharya, 2007), and amphibole-plagioclase-quartz-garnet (Kohn and Spear, 1989, 1990; Dale et al., 2000). The collection is completed with amphibole-melt and amphibole-only thermobarometers (e.g., Helz, 1979; Otten, 1984; Hammarstrom and Zen, 1986; Hollister et al., 1987; Johnson and Rutherford, 1989; Schmidt, 1992; Anderson and Smith, 1995; Ernst and Liu, 1998; Ridolfi et al., 2010; Ridolfi and Renzulli, 2012; Molina et al., 2015; Mutch et al., 2016; Putirka, 2016; Zhang et al., 2017) as well as expressions based on amphibole-saturations surfaces (Molina et al., 2015; Putirka, 2016) that provide valuable constraints on the P-T conditions of amphibole saturation in magmatic systems.

The NaSi–CaAl exchange equilibrium between calcic amphibole and plagioclase, which can be expressed in terms of either tschermakite and glaucophane (e.g., Spear, 1980), *R1*:

$$\underset{(Ts)}{\square Ca_2Mg_3Al_2Al_2Si_6O_{22}(OH)_2} + \underset{(Ab)}{2NaAlSi_3O_8} = \underset{(Gln)}{\square Na_2Mg_3Al_2Si_8O_{22}(OH)_2} + \underset{(An)}{2CaAl_2Si_2O_8}$$

(mineral abbreviations after Whitney and Evans, 2010) or richterite and edenite (e.g., Holland and Blundy, 1994), *R2*:

$$\underset{(Ed)}{NaCa_2Mg_5AlSi_7O_{22}(OH)_2} + \underset{(Ab)}{NaAlSi_3O_8} = \underset{(Rct)}{NaCaNaMg_5Si_8O_{22}(OH)_2} + \underset{(An)}{CaAl_2Si_2O_8}$$

was calibrated as a thermometer by Spear (1980) and Holland and Blundy (1994). The expression of the latter authors has been extensively used to constrain temperature conditions during crystallization of hydrous magmas and during metamorphism of basic to acid rocks (e.g., see reviews in Anderson, 1996, 2008). However, Blundy and Cashman (2008) noted that this expression has systematic errors that were attributed to an inappropriate correction of non-ideality in amphibole. This can cause difficulties in the determination of amphibole stability fields in a large diversity of rock types. The calibration of amphibole-only thermometers, such as those by Ridolfi and Renzulli (2012) and Putirka (2016), might overcome this problem in igneous rocks, but, as will be demonstrated, they also show significant inaccuracies.

It is worth recalling that *accuracy is a necessary condition for an unambiguous interpretation of precision*. This is illustrated in Figure 1a where temperatures estimated with the amphibole-plagioclase thermometer from Holland and Blundy (1994) for 41 experimental data compiled from the literature are plotted against the experimental temperature. For these data, the precision is close to ±50ºC, indicated at 1s level, whereas the regression line of estimated versus experimental temperatures presents a slope of 0.69 and an intercept of 244ºC, thus differing significantly from the one-to-one line that denotes a perfect accuracy. Figure 1a shows that data points lying along the +1s and -1s lines can exhibit a quite different exactitude (note pairs z1-z2 and z3-z4 in Fig. 1a) that depends on the differences between the experimental temperatures and that at the crossing point (ca. 800ºC; Fig. 1a), defined by the interception between the regression line and the one-to-one line (marked by a star in Fig. 1a). So, the points z1 (T(exp) > 800°C) and z3 (T(exp) < 800°C) that lie in the +1s line have a contrasting accuracy: the temperature estimate is perfect for the former, but shows a discrepancy of

+100°C for the latter; the opposite is observed for the corresponding points z2 and z4 located in the -1s line. Similar ambiguities arise when temperature residuals present a significant dependence on mineral composition as shown in Figure 1b where the regression line of temperature residuals for the indicated expression versus amphibole Mg occupancy presents a negative correlation. The crossing point is located at ca. 2.5 apfu Mg (normalization to 23O). Residuals are null for points z5 (Mg > 2.5 apfu) and z8 (Mg < 2.5 apfu) that lie respectively in the +1s and -1s lines, whereas the corresponding points z6 and z7, located respectively in -1s and +1s lines, present absolute residuals of 100ºC.

In this work, we calibrate new expressions of the *amphibole-plagioclase NaSi–CaAl exchange thermometer* using an experimental data set compiled from the literature with 203 amphibole-plagioclase compositional pairs. Calculations were performed by robust regression methods based on multiple maximum-likelihood estimators (MM estimators, Yohai, 1987), which have given successful results in the calibration of amphibole-melt and amphibole-plagioclase thermobarometers (Molina et al., 2015). Various calibration and test data subsets were considered to evaluate the robustness of the derived parameters in the thermodynamic models, and the accuracy and precision of the expressions. We also carry out a test of the performance of the amphibole-plagioclase thermometer of Holland and Blundy (1994 — expression B), and the calibrations of the amphibole-only thermometer of Ridolfi and Renzulli (2012 — expression 2) and Putirka (2016 — expressions 5 and 6). The new thermometric calibrations have an overall precision similar to those of the tested expressions, but show a better accuracy, and hence are suitable for estimating temperature conditions in a wider range of amphibole compositions from igneous and high-grade metamorphic rocks.

Thermodynamic formulation

The thermodynamic basis of *exchange equilibria* — a term introduced in the geologic literature by Ramberg and De Vore (1951) — of atomic species between coexisting mineral phases is given by the equilibrium condition (e.g., Ganguly, 2008):

$$\Delta H_r^o - T\Delta S_r^o + (P - P^o)\Delta V_r^o + RTlnK = 0 \quad (1)$$

where ΔH_r^o, ΔS_r^o and ΔV_r^o are, respectively, the changes in enthalpy, entropy and volume of reaction at standard state T^o and P^o, R is the gas constant (8.3144 $J\,K^{-1}\,mol^{-1}$), and K is the equilibrium constant. It is important to note that the values of ΔH_r^o, ΔS_r^o and ΔV_r^o should be considered more as fitting parameters than as thermodynamic values for the end-member components because they will absorb a fair amount of the assumptions built into this thermodynamic analysis, such as the absence of heat capacities, and coefficients of thermal expansion and compressibility to correct for departures of enthalpy, entropy and volume from the standard state values.

The application of the equilibrium condition to the amphibole-plagioclase NaSi–CaAl exchange reaction *R1* results in:

$$\Delta H_r^o - T\Delta S_r^o + (P - P^o)\Delta V_r^o + RTlnK^{id} + \Delta G_{amp}^{ex} + \Delta G_{pl}^{ex} = 0 \quad (2)$$

where K^{id} is the ideal equilibrium constant expressed as an ionic mixing-on-site solution model:

$$K^{id} = \left(\frac{X_{Si}^{T1} X_{Na}^{M4}}{4X_{Al}^{T1} X_{Ca}^{M4}} \frac{p_{an}}{p_{ab}}\right)^2 \quad (3)$$

(see Table 1 for the definition of site atomic fractions, X_j^s, and molar fractions of end-member components, p_i), and ΔG_{amp}^{ex} and ΔG_{pl}^{ex} are the excess Gibbs free energy of reaction for, respectively, amphibole:

$$\Delta G_{amp}^{ex} = RTln\gamma_{gln} - RTln\gamma_{ts} \quad (4)$$

and plagioclase:

$$\Delta G_{pl}^{ex} = 2RTln\gamma_{an} - 2RTln\gamma_{ab} \quad (5)$$

ΔG_{amp}^{ex} has been formulated using the multisite macroscopic solution model of Powell and Holland (1993) considering the distribution of species □–K–Na–Ca–Mg–Fe^{2+}–Fe^{3+}–Al–Ti–Si over the sites A, M4, M13, M2 and T1 (Table 2). The mixing properties of Cr^{3+}, Mn^{2+}, and the substitution of F^- and Cl^- for OH on the O(3)-site were not considered because of their low occupancies in amphibole from the experimental data set used in this work. Therefore, the derived expressions cannot be used for Cl-rich and/or F-rich amphiboles (compositional ranges in the data set: F < 0.062 apfu, Cl < 0.006 apfu). Ti-rich pargasite and kaersutite, which can be significantly dehydrogenated, were also excluded (Popp and Bryndzia, 1992).

The ΔG_{amp}^{ex} is given from the following expression with 9 linearly independent interaction mixing parameters (Table 3):

$$\Delta G_{amp}^{ex} = W_0 + \sum_{i=1}^{8} p_i W_i \tag{6}$$

where the W_i parameters are allowed to be pressure and temperature dependent:

$$W_i = W_i^H - TW_i^S + PW_i^V \tag{7}$$

Introducing 6 and 7 in expression 2 we obtain after some algebraic manipulations:

$$-\left(RTlnK^{id} + \Delta G_{pl}^{ex}\right) = \Delta H_r^o + W_0^H - P^o \Delta V_r^o - T(\Delta S_r^o + W_0^S) + P(\Delta V_r^o + W_0^V) + \sum_{i=1}^{8} \{p_i W_i^H - p_i T W_i^S + p_i P W_i^V\} \tag{8}$$

that can be expressed in a more compact way as:

$$-\left(RTlnK^{id} + \Delta G_{pl}^{ex}\right) = A - TB + PC + \sum_{i=1}^{8} \{p_i W_i^H - p_i T W_i^S + p_i P W_i^V\} \tag{9}$$

where: $A = \Delta H_r^o + W_0^H - P^o \Delta V_r^o$, $B = \Delta S_r^o + W_0^S$ and $C = \Delta V_r^o + W_0^V$.

This expression was used for retrieving A, B, C, and amphibole mixing parameters with ΔG_{pl}^{ex} fixed using two different approaches (Table 4): 1) the ternary feldspar solution model of Elkins and Grove (1990), $\Delta G_{pl}^{ex}(EG90)$, and 2) the simplified version of the Darken's Quadratic Formalism (DQF) for plagioclase of Holland and Powell (1992), $\Delta G_{pl}^{ex}(HP92)$.

Once the reaction parameters and the amphibole mixing parameters had been retrieved, the following thermometric expression was derived by solving for temperature in relation 9:

$$T = \frac{-[\Delta G_{pl}^{ex} + A + PC + \sum_{i=1}^{8} \{p_i W_i^H + p_i P W_i^V\}]}{RlnK^{id} - B - \sum_{i=1}^{8} p_i W_i^S} \tag{10}$$

that requires iterative calculations for temperature determinations because of the temperature dependence of the G_{pl}^{ex} term (see further comments below).

Compositional data set

We have created an amphibole-plagioclase compositional data set for this study with experiments compiled from LEPR (Hirschmann et al., 2008) and other published works (see Appendix A from the electronic supplementary material). To minimize problems related to the achievement of equilibrium, only experimental data with the following run durations were chosen: > 180 h at 600-650°C, > 150 h at 650-700°C, > 100 h at 700-800°C, > 50 h at 800-900°C and > 20 h at 900-1000°C.

The Full Data Set (FDS) contains 203 compositional pairs that encompass a P-T range from 1 to 15 kbar and from 640 to 1000ºC (see also Table 1SB from Appendix B in the electronic supplementary material for a summary). The amphibole-plagioclase assemblages can also contain quartz (26% of the experiments), orthopyroxene (29%), clinopyroxene (25%), olivine (7.9%) and garnet (7.9%); 8.4% of the experiments are subsolidus (Appendix A).

Mineral chemistry

Amphibole

There have been proposed many amphibole normalization schemes for thermobarometric calculations (e.g., Anderson, 1996; Almeev et al., 2002; Ridolfi and Renzulli, 2012; Molina et al., 2015; Putirka, 2016; Li et al., 2019). In this work, amphibole formula was calculated on the basis of 23 oxygen atoms with ferric/ferrous iron ratios calculated using a modified version of the average Fe^{3+} method of Spear and Kimball (1984) proposed by Holland and Blundy (1994). The method, corrected for some minor mistakes detected in the previous formulation, is described in Appendix A from Dale et al. (2005); Fe^{3+}/Fe_T ratios estimated by this method present a reasonable agreement with wet chemical analyses from an extensive calcic amphibole data set compiled by Leake (1968) — see Fig. 14 in Dale et al. (2005). Amphibole OH contents were calculated assuming F + Cl + OH = 2.

The experimental data set comprises mostly magnesiohornblende (40% of the data), magnesiohastingsite (19%), pargasite (11%), and tschermakite (11%), and minor amounts of edenite, ferrohornblende, ferropargasite and ferrotschermakite, which represent, altogether, ca. 10% of the total (classification after Leake et al., 1997); in addition, there are also 9.4% of subcalcic amphibole. Amphibole compositions have 0.57-2.04 apfu Al^{IV}, < 0.35 apfu Ti, 1.29-1.87 apfu Ca, 0.067-0.427 apfu Na^{M4}, 0.078-0.80 apfu A-site occupancy and $Mg/(Mg+Fe^{2+})$ and Fe^{3+}/Fe_T ratios of 0.35–0.93 and 0.04-0.70 respectively (Figs. 2a-d; Table 1SB).

Plagioclase

The composition of plagioclase in the experimental data set is mostly andesine (41%), labradorite (33%) and bytownite (20%), with minor amounts of oligoclase (6%) (Fig. 3a). The abundance of orthoclase component is < 11 mol% (Fig. 3b).

Regression and outlier detection methods

The reaction parameters and the amphibole mixing parameters were retrieved by robust regression methods based on multiple maximum-likelihood estimators (MM-estimators; Yohai, 1987) using the "mmregress" command, implemented in Stata software by Verardi and Croux (2009), setting efficiency at 0.7 and invoking the "initial" option. Selection of independent variables (i.e., the amphibole mixing parameters and the reaction parameters) was carried out using forward selection and backward elimination procedures; the variables were considered significant, and hence included in the model, when t-values of the estimated coefficients were >|3.7|, what assures $P(>|t|) = 0$.

Detection of vertical outliers and leverage points was carried out using a plot (Fig. 4) of robust standardized residuals versus Mahalanobis distance. Threshold values for considering data as outliers were set to −2.25 and +2.25 for the standardized residuals — these limits are the values of the standard normal distribution that differentiate the 2.5% remotest area of the distribution from the central mass

(Verardi and Croux, 2009) — and to $\sqrt{\chi^2_{p,0.975}}$ (where p is the number of regression parameters) for the Mahalanobis distance (see Verardi and Croux, 2009).

The precision and accuracy of the derived thermometers were evaluated by fitting the relationships between calculated, $\hat{T}_i$, and experimental, T_i, temperatures using ordinary least squares (OLS) regression methods on the full data set, and the calibration and test data sets (see below for details). Absence of systematic errors was evaluated by checking whether the linear relation between these variables, $\hat{T}_i = a + b\,T_i$, is significantly indistinguishable from the one-to-one relation: $\hat{T}_i = T_i$. This was done by estimating the closeness of the slope to 1 and performing a t-test on the constant term.

The precision of the thermometric expressions for each data set was estimated using the root-mean-square errors (RMSE) obtained by OLS regression (e.g., see Putirka, 2008, and Molina et al., 2015). Besides, the precision given by the average absolute deviation (AAD; e.g., Blundy and Cashman, 2008) and the median absolute deviation (MAD) is also reported in Tables 2SB-6SB for comparison.

Calibration of new expressions of the amphibole-plagioclase NaSi–CaAl exchange thermometer

We derived thermodynamic models for expression 9 using a data set with the maximum number of observations (Calibration Data Set 1, CDS1, see Appendix C from the electronic supplementary material for details) that behaved well, i.e., without outliers in the models. The accuracy and precision of the thermometers derived from these models using expression 10 were tested on the CDS1 and FDS, which also includes the outlying data. On the other hand, it is customary to test thermobarometric expressions on an independent data set (e.g., see different approaches in Holland and Blundy, 1994, and Putirka, 2016) to assess how well the expressions perform for data not included in the calibration. Therefore, we split the data set in approximately two halves, Calibration Data Set 2 (CDS2) and Test Data Set 2 (TDS2), including in the former experimental data that were consistent with the models found with CDS1 (Appendixes A and C). CDS2 was used for deriving extra models with the same fitting parameters as those obtained with CDS1, thus making it possible to evaluate the influence of the number of data on the retrieved values of the parameters. Accuracy and precision for the thermometric expressions derived from these extra models were evaluated with CDS2, TDS2 and FDS.

The reaction parameters and the amphibole mixing parameters obtained with MM-estimators are listed in Table 5. Models A1 and B1 were calculated using CDS1 (196 observations after removing 7 vertical outliers and leverage points in the diagnostic plots; Fig. 4), whereas CDS2 (92 observations after removing 12 vertical outliers and leverage points in the diagnostic plots; Fig. 4) was used for models A2 and B2; it was employed $\Delta G_{pl}^{ex}(EG90)$ for A1 and A2, and $\Delta G_{pl}^{ex}(HP92)$ for B1 and B2. The models have significant values for the amphibole mixing parameters W_2^H, W_5^H, W_7^S and W_8^S (Table 5). The reaction parameters *A* and *B* are also significant in the four models; however, the *C* parameter does not satisfy the selection criteria and was set to zero; this is in agreement with a null reaction volume estimated by Holland and Blundy (1994) for the equivalent reaction *R2*.

The expressions present absolute t-values higher than 4 for all the accepted parameters, but W_7^S in model A1 that is close to 3.7 (Table 5); however, all of them are significant with $P(>|t|) = 0$. The scale parameters for models A1 and B1 are very close varying between 6348 and 6361 J, whereas those for models A2 and B2 are up to ca. 1900 J lower (range: 4475-4634 J). The parameters in the models obtained with a single data set show very close fitted values despite using different plagioclase mixing models. Besides, differences between the four models for *A, B* and W_5^H parameters are within uncertainties indicating a negligible dependence on the used data set. However, the differences for the enthalpic W_2^H and entropic W_7^S and W_8^S parameters are slightly higher, reaching up to 12100 J, and 48 and 26 J/K, respectively. The estimated values for the entropic *B* parameter are ca. 90-94 J/K, which are close, within uncertainties (±11-20 J/K), to those reported by Spear (1980; range: 67-93 J/K), and by Holland and Blundy (1994) for the equivalent reaction *R2* (72 J/K). It is important to note that the

DOI: https://doi.org/10.2138/am-2021-7400. http://www.minsocam.org/

terms *A, B* and *C,* aside from the fact that they include the W_0^H, W_0^S and W_0^V parameters, could not be considered energy parameters representative of the end-member reaction because, as indicated by Holland and Blundy (1994), they also accommodate any deficiency and simplification of the models.

The thermometric expressions for the four models obtained by substituting the derived parameters in expression 10 are as follows (temperature in degrees Celsius):

$$T_{A1} = -\frac{G_{pl}^{ex}(EG90) - 2.80\ 10^4\ p_2 + 7.31\ 10^4\ p_5 + 1.36\ 10^5}{-101\ p_7 - 72\ p_8 - 90 + R\ln K^{id}} - 273 \tag{11a}$$

$$T_{B1} = -\frac{G_{pl}^{ex}(HP92) - 3.02\ 10^4\ p_2 + 7.08\ 10^4\ p_5 + 1.40\ 10^5}{-109\ p_7 - 70\ p_8 - 91 + R\ln K^{id}} - 273 \tag{11b}$$

$$T_{A2} = -\frac{G_{pl}^{ex}(EG90) - 3.77\ 10^4\ p_2 + 6.96\ 10^4\ p_5 + 1.477\ 10^5}{-132\ p_7 - 96\ p_8 - 94 + R\ln K^{id}} - 273 \tag{11c}$$

$$T_{B2} = -\frac{G_{pl}^{ex}(HP92) - 4.01\ 10^4\ p_2 + 7.04\ 10^4\ p_5 + 1.48\ 10^5}{-149\ p_7 - 93\ p_8 - 94 + R\ln K^{id}} - 273 \tag{11d}$$

The test of all the new amphibole-plagioclase thermometric expressions, but B1, carried out on CDS1, CDS2, TDS2 and FDS demonstrates a good performance with calculated versus experimental temperatures statistically indistinguishable from the one-to-one line (Figs. 5a-d; Table 2SB). The precision for expression A1 given by RMSE is ±50°C for CDS1 and ±55°C for FDS. Expressions A2 and B2 yield a RMSE precision for CDS2 of ±35-36°C, being the uncertainty 16°C higher for the TDS2 and 20°C higher for the FDS.

The residuals for the four new expressions show no important dependence on mineral compositions (Figs. 1SB and 2SB in Appendix B), except for a slight positive correlation with amphibole Na^{M4} occupancy and anorthite content of plagioclase (Figs. 6 and 7). For this reason, more accurate temperature estimates for expressions A1, A2 and B2 are expected if $Na^{M4} < 0.30$ apfu, with the additional restriction of $p_{an} < 0.80$ for B2 — compositional limits obtained by fixing threshold values for the average residuals, as estimated by the regression lines of residuals versus mineral compositions, of ±25-30°C (i.e., ca. one half of the RMSE precision yielded by the expressions for the FDS).

Because of the absence of a significant reaction volume in the models proposed for *R1*, expressions B1 and B2 are pressure independent, whereas the expressions A1 and A2 could have some pressure dependence due to the non-null volumetric terms present in the mixing parameters $W_{an\,or}$, $W_{ab\,or}$, $W_{or\,ab}$ and $W_{or\,ab\,an}$ from $\Delta G_{pl}^{ex}(EG90)$, but it is expected to be very small as a consequence of the low orthoclase content of plagioclase that can be used in the calculations (see below for requirements of use of the amphibole-plagioclase thermometric expressions).

In order to estimate temperatures with the derived expressions, it is necessary to perform a tedious algebraic computation that involves iterative calculations because of the temperature dependence of the G_{pl}^{ex} term. To facilitate calculations, an Excel spreadsheet downloadable from the electronic supplementary material (Appendix D) has been programmed that calculates amphibole and plagioclase formulas from oxides, and determines temperatures with the new thermometric expressions. The Excel spreadsheet also estimates pressures with the barometer from Molina et al. (2015) based on the Al-Si partitioning between amphibole and plagioclase.

Test of amphibole-based thermometers

The precision and accuracy of the amphibole-plagioclase thermometer from Holland and Blundy (1994 — expression B) and the amphibole-only thermometers from Ridolfi and Renzulli (2012 — expression 2) and Putirka (2016 — expressions 5 and 6) are assessed in this section. In order to evaluate how the number of observations influences the behavior of the expressions we have performed the statistical test on data sets FDS, CDS2, and TDS2. For each data set, we selected only the subsets of data that satisfy the compositional restrictions of use of the calibrations (expression B: p_{an} = 0.10-0.90, Na^{M4} > 0.06 apfu, Al^{VI} < 1.81 apfu, and Si = 6.0-7.7 apfu; expression 2: $Mg/(Mg+Fe^{2+})$ > 0.5; expressions 5 and 6: no compositional restrictions). In addition, given that our main task is to determine equilibrium temperatures in natural assemblages, i.e., temperature is the unknown, we are also interested in evaluating how the thermometric expressions extrapolate outside the temperature range of each calibration; therefore, for each data set we distinguished two subsets: one with the full temperature range (FTR; 640-1000°C) and the other with the calibration temperature range of each expression (CTR; expression B: T = 500-900ºC; expression 2: T > 800°C; expressions 5 and 6: T > 700°C).

Amphibole-plagioclase thermometer

The calibration B from Holland and Blundy (1994) of the amphibole-plagioclase thermometer is based on the exchange equilibrium *R2*. It uses the DQF plagioclase solution model from Holland and Powell (1992) to account for non-ideal mixing in plagioclase, and the formulation of the multisite macroscopic solution model of Powell and Holland (1993) for retrieving the mixing parameters of amphibole. The proposed expression, which presents 6 parameters (one of them pressure-dependent), was calibrated using a data set with 250 amphibole-plagioclase pairs of which 92 are experimental and 158 are natural; a precision of ca. ±40ºC was reported for this calibration.

The test carried out on all the subsets but the CTR subset from TDS2 reveals significant inaccuracies with regression lines of estimated versus experimental temperatures having slopes of 0.64-0.71 and intercepts at 226-268°C (Table 3SB); this leads to average temperature underestimations, as indicated by the regression lines of estimated versus experimental temperatures, of 40-60°C at 900°C and ca. 80°C at 1000°C (Fig. 8a). The precision given by RMSE for these data sets ranges between ±51-67ºC. By contrast, the CTR subset from TDS2 yields more accurate temperature estimates with relations of estimated versus experimental temperatures closer to the one-to-one line (Fig. 8a; Table 3SB); however, the precision is poor (±72ºC).

Blundy and Cashman (2008) noted that the residuals have an important negative correlation with the amphibole Mg/(Mg+Fe^{2+}) ratio. Accordingly, the residuals for each data set show a systematic negative correlation with Mg occupancy (and positive with Fe^{2+}, not shown) ranging average residuals, as estimated by the regression lines of residuals versus mineral compositions, from -50 to -90°C for high-Mg compositions (Mg = 4 apfu; Fig. 9); at the other compositional end (Mg = 1.5 apfu), temperature discrepancies can be lower varying average residuals from 10 to 75°C. However, the test performed for this expression also evidences a significant dependence of residuals on amphibole Na^{M4} and Fe^{3+} occupancies and plagioclase composition (Fig. 9). So, the residuals have an important negative correlation with Na^{M4} for the subsets of TDS2 and FDS, thus giving the latter average residuals ranging between -55 and -75°C for Na^{M4} = 0.4 apfu; however, for the two CDS2 subsets, they show a negligible dependence, emphasizing the interplay of multiple factors on the reliability of the expression. In a similar way, the relationships of residuals versus Fe^{3+} occupancy also suggest a relatively good behavior for the two CDS2 subsets and a systematic variation for the TDS2 subsets resulting in global average residuals given by the FDS subsets of up to ca. -50°C for low-Fe^{3+} amphibole (Fe^{3+} = 0.1 apfu); for high-Fe^{3+} amphibole, temperature discrepancies are, on average, less important. The residuals for the three CTR subsets show a positive correlation with anorthite content ranging average residuals from -25 to -60°C for oligoclase with p_{an} = 0.20, and from 20 to 30°C for bytownite with p_{an} = 0.85. However, the plagioclase composition dependence of residuals is negligible when considering the FTR subsets, clustering average residuals between -10 and -30°C.

Amphibole-only thermometers

The amphibole-only thermometers are based on empirical temperature-amphibole composition relationships. The expression 2 by Ridolfi and Renzulli (2012), which includes 8 amphibole compositional parameters, one pressure-dependent term and one constant term, was calibrated using 61 experimental data and yielded a precision of ±25ºC (tested using only the calibration data set). The expression 5 by Putirka (2016), which is pressure-independent and has four amphibole compositional parameters and one constant term, was calibrated using 156 experimental data and yielded a precision ranging from ±30ºC (calibration data set) to ±53ºC (test data set with 392 experimental data). This author also calibrated expression 6 with an additional pressure-dependent term that did not significantly improve the precision (a reduction in errors of only 1-2°C).

Expressions 2, 5 and 6 are widely used for estimating amphibole crystallization temperatures in igneous rocks, however the test done on the experimental data sets evidences a poor performance (Tables 4SB-6SB). Thus, they are more inaccurate than the expression B from Holland and Blundy (1994), showing slopes for regression lines of estimated versus experimental temperatures ranging between 0.33-0.53 in expression 2, 0.30-0.75 in expression 5 and 0.27-0.71 in expression 6; their intercepts are very much higher than those for expression B, with values ranging between 421-641°C in expression 2, 218-632°C in expression 5, and 250-656°C in expression 6. Accordingly, temperatures can be, on average, overestimated at 650°C by ca. 140-160°C with expression 2 and 80-180°C with expressions 5 and 6 (Figs. 8b-d). The precision given by RMSE ranges between ±33-51°C in expression 2, ±41-52°C in expression 5 and ±41-53°C in expression 6.

The residuals for the three expressions present a significant dependence on amphibole Al^{VI} and Mg (also Fe^{2+}, not shown) occupancies (Figs. 10a-c). Temperatures are significantly overestimated for high-Al^{VI} amphibole, yielding the test on FTR subsets from CDS2 and FDS average residuals > 160°C for amphibole with > 1.2 apfu Al^{VI}. Temperatures tend to be also overestimated in low-Mg amphibole with average residuals > 100°C for expression 2 and > 70°C for expressions 5 and 6 in amphibole with < 2 apfu Mg from the indicated FTR subsets.

Discussion

Shortcomings in the modeling of amphibole solid solutions: prerequisites for use of the amphibole-plagioclase thermometric calibrations

An accurate and precise determination of the mixing properties of multicomponent calcic amphibole is hampered, aside from short-range order (e.g., Hawthorne and Della Ventura, 2007) and phase transitions (e.g., Welch et al., 2007), by the complexity of long-range order that controls the distribution of cations over sites (Oberti et al., 2007). These authors have shown that it is significantly more complex than the scheme adopted in this work (Table 2), and normally assumed in the thermodynamic treatment of amphibole solid solutions (e.g., Blundy and Holland, 1990; Mäder and Berman, 1992; Will and Powell, 1992; Holland and Blundy, 1994; Dale et al., 2000, 2005; Bhadra and Bhattacharya, 2007; Diener et al., 2007; Chambers and Kohn, 2012; Diener and Powel, 2012; Green et al., 2016). Accordingly, Oberti et al. (2007, and references therein) indicated that octahedral Al is partly disordered over M2 and M3 sites in pargasites and that Al occupancy in M3 site increases with Mg content, whereas tetrahedral Al is partly disordered over the T1 and T2 sites not only in subsilicic, ferri-ferrosadanagaites but also in magnesiohornblendes and pargasites. These authors also reported the presence of Ti and Fe^{3+} in all the M1, M2, and M3 sites.

The distribution of Fe^{2+} and Mg^{2+} over M1, M2, M3 and M4 sites presents additional difficulties (Oberti et al., 2007). It is well understood in *cummingtonite–grunerite series* (e.g., Ganguly, 1982; Hirschman et al., 1994; Ghiorso et al., 1995) and *tremolite–ferro-actinolite series* (e.g., Evans and Yang, 1998; Driscall et al., 2005), thus leading to the calibration of accurate solutions models in the Ca-Mg-Fe^{2+} amphibole quadrilateral (Ghiorso and Evans, 2002). However, it remains largely unknown in pargasitic and tschermakitic amphiboles (see Oberti et al., 2007, for further details).

It is important to note that long-range order affects not only the formulation of the ideal activity but also the number of independent amphibole phase components to be considered in the contribution of the excess Gibbs free energy. Therefore, without a precise understanding of the behavior of long-range order as a function of pressure, temperature and amphibole composition, the thermodynamic treatment of multicomponent amphibole solid solutions will be only approximated. Under these circumstances, we expect that the thermobarometric expressions derived from these simple solution models will work well for amphiboles whose compositions match as much as possible those of the calibration data set. For this reason, it is essential to evaluate the critical parameters and their threshold values that delimit the optimal compositional region of application of the thermometric expressions.

For the amphibole-plagioclase thermometric expressions derived in this work, we found the following restrictions of use: 1) *amphibole composition*: Na^{M4} = 0.06-0.50 apfu, Ca > 1.2 apfu, Ti < 0.4 apfu, K < 0.25 apfu, and $p_9 < 0.34$ (tremolite phase component, see Table 1); 2) *plagioclase composition*: $p_{an} > 0.18$ and $p_{or} < 0.11$; and 3) *denominator values in expression 5, Den(Exp.)*: Den(A1) = -182 – -122, Den(A2) = -195 – -130 and Den(A2) = -195 – -130. Besides, given the slight dependence of temperature residuals on anorthite content of plagioclase and amphibole Na^{M4} occupancy, to guarantee more accurate results we recommend using them to amphibole with Na^{M4} < 0.30 apfu, limiting also the application of expression B2 to $p_{an} < 0.80$.

Applications of amphibole-plagioclase and amphibole-only thermometry to igneous and high-grade metamorphic rocks

The new calibrated thermometers (all expressions, but B1 that is less accurate) and the calibrations from Holland and Blundy (1994), Ridolfi and Renzulli (2012) and Putirka (2016) are applied to natural amphibole-plagioclase assemblages in this section to evaluate how the reported inaccuracies affect temperature estimations. The use of the amphibole-only thermometers was restricted to igneous rocks as they were calibrated for supersolidus assemblages, whereas the amphibole-plagioclase thermometers were applied to both igneous and high-grade metamorphic rocks.

For this purpose, we selected case studies from four *metamorphic complexes*: 1) amphibolites and mafic granulites from the Berit meta-ophiolite, SE Anatolia; 2) HP-Grt granulites from Kvalvåg, Kristiansund area, Norwegian Caledonides; 3) Opx-Cpx amphibolites and Cpx-poor amphibolites from the Connaughton Terrane, central Western Australia; and 4) amphibolites from the Archean Fiskenæsset complex, SW Greenland; and five *igneous associations*: 1) andesites from the catastrophic 1956 eruption of the Bezymyannyi volcano, Kamchatka; 2) Hbl gabbros and diorite enclaves from the

Val Fredda Complex, Tertiary Adamello Massif; 3) gabbro-diorites, metadiorites and granodiorites from the Mesozoic Barcroft granodioritic pluton, central White Mountains; 4) cortlandtites from the appinite suite of the Variscan Avila batholith, Central Iberian Zone; and 5) Ol hornblendites from the sheeted sills at Onion Valley, Mesozoic Sierra Nevada batholith — see Tables 7SB and 8SB for data sources and a brief description of petrography and geological setting.

The composition of 62 selected amphibole-plagioclase pairs and temperature estimates calculated with the indicated thermometric expressions are reported in Appendix E from the electronic supplementary material. Calculations for expressions B, 2 and 6 were carried out at the pressure ranges indicated by the authors, and at fixed pressures of 1 and 15 kbar for expressions A1 and A2 as they show a negligible pressure dependence — indeed, temperature discrepancies are < 2ºC for all data but one with a value of 8ºC, see Appendix E; expressions B2 and 5 are pressure independent. The average values of temperatures estimated at the indicated pressure ranges are used in the following discussion. Discrepancies between average temperature estimates obtained by the new calibrated thermometers and expressions B2, 2, 5 and 6 are displayed in Figures 11-13. An overall precision of ±50ºC, indicated at 1s level, is assumed for all expressions.

Temperature discrepancies between the new calibrations and that from Holland and Blundy (1994) for both igneous and metamorphic assemblages are, in general, within the ±2s interval and show a negative correlation with the temperature estimated with the new calibrations and with amphibole Mg and Na^{M4} occupancies and a positive correlation with amphibole Fe^{3+} occupancy (Figs. 11-12). These relationships are similar to those observed in the test performed on the experimental data sets, being therefore likely that the discrepancies are caused by the inaccuracies detected in the expression B from Holland and Blundy (1994). Likewise, temperature discrepancies between the new calibrations and those by Ridolfi and Renzulli (2012) and Putirka (2016), which can be higher reaching >+2s in ca. 20 % of the data (Fig. 13), can also be attributed to the inaccuracies reported in the amphibole-only expressions as their relationships with amphibole composition are akin to those observed with the experimental data, thus overestimating temperatures in amphibole with either high Al^{VI} or low Mg occupancies.

Therefore, we recommend using the new calibrations as their accuracy is significantly better within the prescribed compositional limits of use; amphibole-only thermometry should be only applied to high-Mg amphibole that might have more likely crystallized at high temperatures (e.g., amphibole primocrysts from hornblendites, gabbros, diorites, basalts and andesites).

Implications

In spite of the complexity of cation distributions over amphibole sites (Oberti et al., 2007), robust regression methods based on MM-estimators (Yohai, 1987) make it possible to calibrate, almost pressure independent, expressions for the amphibole-plagioclase NaSi–CaAl exchange thermometer using the formulation of the multisite macroscopic solution model of Powell and Holland (1993) to correct for ideality deviations in the calcic amphibole solid solution. These expressions present an overall precision of ca. ±50ºC that is close to those reported for the calibration B of the amphibole-plagioclase thermometer by Holland and Blundy (1994), and the calibrations 2 by Ridolfi and Renzulli (2012), and 5 and 6 by Putirka (2016) of the amphibole-only thermometer. However, the new expressions are significantly more accurate, *a condition required for an unambiguous interpretation of precision*, yielding better results than the calibration B for high-Mg amphibole, and the calibrations 2, 5 and 6 for amphibole with either low Mg or high Al^{VI} occupancies. Indeed, these latter only give accurate results in high-Mg amphibole that most likely crystallized at temperatures >800ºC. Amphibole Na^{M4} and Fe^{3+} occupancies can also affect significantly the accuracy of expression B.

The new calibrations can be used for calculating amphibole-plagioclase equilibrium temperatures for a large diversity of amphibole-plagioclase assemblages from igneous and high-grade metamorphic rocks that satisfy the following restrictions that delimit the optimal region of use: 1) *amphibole* *composition*: Na^{M4} = 0.06-0.50 apfu, Ca > 1.2 apfu, Ti < 0.4 apfu, K < 0.25 apfu, and $p_9 < 0.34$; 2) *plagioclase composition*: $p_{an} > 0.18$ and $p_{or} < 0.11$; and 3) *Den(Exp.) parameter*: Den(A1) = -182 – -122, Den(A2) = -195 – -130 and Den(A2) = -195 – -130. Besides, small orthoclase contents ($p_{or} < 0.11$) are required to guarantee a negligible pressure dependence of expressions A1 and A2, whereas more accurate results would be obtained with the three expressions if $Na^{M4} < 0.30$ apfu, being required for B2 the additional restriction of $p_{an} < 0.80$.

Acknowledgments

We thank Saskia Erdmann and David Jenkins for the thorough revision of the manuscript and for their insightful comments. We are grateful to Renat Almeev for his comments and efficient and helpful editorial handling. This work has been financed by the grants CGL2013-40785-P (Ministerio de Economía y Competitividad, Gobierno de España) and P12.RNM.2163 (Junta de Andalucía).

References cited

Almeev, R.R., Ariskin, A.A., Ozerov, A.Y., and Kononkova, N.N. (2002) Problems of the stoichiometry and thermobarometry of magmatic amphiboles: An example of hornblende from the andesites of Bezymianny volcano, Eastern Kamchatka. Geochemistry International, 40, 723–738.

Anderson, J.L. (1996) Status of thermobarometry in granitic batholiths. Transactions of the Royal Society of Edinburgh: Earth Sciences, 87, 125–138.

Anderson, J.L., and Smith, D.R. (1995) The effects of temperature and fO_2 on the Al-in-hornblende barometer. American Mineralogist, 80, 549–599.

Anderson, J.L., Barth, A.P., Wooden, J.L., and Mazdab, F. (2008) Thermometers and thermobarometers in granitic systems. Reviews in Mineralogy and Geochemistry, 69, 121–142.

Apted, M.J., and Liou, J.G. (1983) Phase relations among greenschist, epidote-amphibolite and amphibolite in a basaltic system. American Journal of Science, 283A, 328-354.

DOI: https://doi.org/10.2138/am-2021-7400. http://www.minsocam.org/

Awalt, M.B., and Whitney, D.L. (2018) Petrogenesis of kyanite- and corundum-bearing mafic granulite in a meta-ophiolite, SE Turkey. Journal of Metamorphic Geology, 36, 881–904.

Bhadra, S., and Bhattacharya, B. (2007) The barometer tremolite + tschermakite + 2 albite = 2 pargasite + 8 quartz: constraints from experimental data unit silica activity, with applications to garnet-free natural assemblages. American Mineralogist, 92, 491–502.

Blundy, J., and Cashman, K. (2008) Petrologic reconstruction of magmatic system variables and processes. Reviews in Mineralogy and Geochemistry, 69, 179–239.

Blundy, J.D., and Holland, T.J.B. (1990) Calcic amphibole equilibria and a new amphibole-plagioclase geothermometer. Contributions to Mineralogy and Petrology, 104, 208–224.

Bucher, K., and Grapes, R. (2011) Petrogenesis of metamorphic rocks. Springer-Verlag, Berlin-Heiderberg.

Castro, A. (2013) Tonalite-granodiorite suites as cotectic systems: A review of experimental studies with applications to granitoid petrogenesis. Earth-Science Reviews, 124, 68–95.

Chambers, J.A., and Kohn, M.J. (2012) Titanium in muscovite, biotite, and hornblende: Modeling, thermometry and rutile activities in metapelites and amphibolites. American Mineralogist, 97, 543–555.

Conrad, W.K., Nicholls, I.A., and Wall, V.J. (1988) Water-saturated and -undersaturated melting of metaluminous and peraluminous crustal compositions at 10 kbar: evidence for the origin of silicic magmas in the Taupo volcanic zone, New Zealand, and other occurrences. Journal of Petrology, 29, 765–803.

Czamanske G.K., and Wones D.R. (1973) Oxidation during magmatic differentiation, Finnmarka complex, Oslo area, Norway: part 2: the mafic silicates. Journal of Petrology, 14, 349–380.

Dale, J., Holland, T., and Powell, R. (2000) Hornblende–garnet–plagioclase thermobarometry: a natural assemblage calibration of the thermodynamics of hornblende. Contributions to Mineralogy and Petrology, 140, 353–362.

Dale, J., Powell, R., White, R. W., Elmer, F. L., and Holland, T. J.B. (2005) A thermodynamic model for Ca–Na clinoamphiboles in Na_2O–CaO–FeO–MgO–Al_2O_3–SiO_2–H_2O–O for petrological calculations. Journal of Metamorphic Geology, 23, 771–791.

Diener, J.F.A., and Powell, R. (2012) Revised activity–composition models for clinopyroxene and amphibole. Journal of Metamorphic Geology, 30, 131–142.

Diener, J.F.A., Powell, R., White, R.W., and Holland, T.J.B. (2007) A new thermodynamic model for clino- and orthoamphiboles in Na_2O–CaO–FeO–MgO–Al_2O_3–SiO_2–H_2O–O. Journal of Metamorphic Geology, 25, 631–656.

Driscall, J., Jenkins, D.M., Dyar, M.D., and Bozhilov, K.N. (2005) Cation ordering in synthetic low-calcium actinolite. American Mineralogist, 90, 900–911.

Elkins, L.T., and Grove, T.L. (1990) Ternary feldspar experiments and thermodynamic models. American Mineralogist, 75, 544–559.

Ernst, W.G. (2002) Paragenesis and thermobarometry of Ca-amphiboles in the Barcroft granodioritic pluton, central White Mountains, eastern California. American Mineralogist, 87, 478–490.

Ernst, W.G., and Liu, J. (1998) Experimental phase-equilibrium study of Al- and Ti-contents of calcic amphibole in MORB – A semiquantitative thermobarometer. American Mineralogist, 83, 952–969.

Evans, B.W., and Yang, H. (1998) Fe-Mg order-disorder in tremolite-actinolite-ferro-actinolite at ambient and high temperatures. American Mineralogist, 83, 458–475.

Fershtater, G.B. (1990) Empirical hornblende-plagioclase geobarometer. Geokhimiya 3, 328–335.

Ganguly, J. (1982) Mg-Fe order-disorder of ferromagnesian silicates. II. Thermodynamics, kinetics, and geological applications. In: Saxena SK (ed) Advances in physical geochemistry. Springer, 2, 58–99.

Ganguly, J. (2008) Thermodynamics in earth and planetary sciences. Springer-Verlag, Berlin.

García-Casco, A., Lázaro C., Rojas-Agramonte, Y., Kröne , A., Torres-Roldán R.L., Núñe K., Millá , G., Neubauer, F., Blanco-Quintero, I. (2008) Partial melting and counter- clockwise P–T path of subducted oceanic crust (Sierra del Convento mé ange, Cuba). Journal of Petrology, 49, 128–161.

Ghiorso, M.S., and Evans, B.W. (2002) Thermodynamics of the amphiboles: Ca–Mg–Fe^{2+} quadrilateral. American Mineralogist, 87, 79–98.

Ghiorso, M.S., Evans, B.W., Hirschmann, M.M., and Yang, H. (1995) Thermodynamics of the amphiboles: Fe-Mg cummingtonite solid solutions. American Mineralogist, 80, 502–519.

Graham, C.M., and Powell, R. (1984) A garnet-hornblende geothermometer: calibration, testing, and application to the Pelona Schist, southern California. Journal of Metamorphic Geology, 2, 13–21.

Green, E.C.R., White, R.W., Diener, J.F.A., Powell, R., Holland, T.J.B., and Palin, R.M. (2016) Activity-composition relations for the calculation of partial melting equilibria in metabasic rocks. Journal of Metamorphic Geology, 34, 845– 869.

Hammarstrom, J.M., and Zen, E. (1986) Aluminum in hornblende: an empirical igneous geobarometer. American Mineralogist, 71, 1297–1313.

Hawthorne, F.C., and Della Ventura, G. (2007) Short-range order in amphiboles. Reviews in Mineralogy and Geochemistry, 67, 173–222.

Helz, R.T. (1979) Alkali exchange between hornblende and melt: a temperature-sensitive reaction. American Mineralogist, 64, 953–965.

Hirschmann, M., Evans, B.W., and Yang, H. (1994) Composition and temperature dependence of Fe-Mg ordering in cummingtonite-grunerite as determined by X-ray diffraction. American Mineralogist, 79, 862–877.

Hirschmann, M.M., Ghiorso, M.S., Davis, F.A., Gordon, S.M., Mukherjee, S., Grove, T.L., Krawczynski, M., Medard, E., and Till, C.B. (2008) Library of experimental phase relations (LEPR): a database and web portal for experimental magmatic phase equilibria data. Geochemistry, Geophysics, Geosystems, 9, Q03011, DOI: 10.1029/2007GC001894.

Holland, T., and Blundy, J. (1994) Non-ideal interactions in calcic amphiboles and their bearing on amphibole-plagioclase thermometry. Contributions to Mineralogy and Petrology, 116, 433–447.

Holland T.J.B., and Powell R. (1992) Plagioclase feldspars: activity-composition relations based upon Darken's Quadratic Formalism and Landau theory. American Mineralogist, 77, 53–61.

Hollister, L.S., Grissom, G.C., Peters, E.K., Stowell, H.H., and Sisson, V.B. (1987) Confirmation of the empirical correlation of Al in hornblende with pressure of solidification of calc-alkaline plutons. American Mineralogist, 72, 231–239.

Johnson, M.C., and Rutherford, M.J. (1989) Experimental calibration of an aluminum-in-hornblende geobarometer applicable to Long Valley caldera (California) volcanic rocks. Geology, 17, 837–841.

Kohn, M.J., and Spear, F.S. (1989) Empirical calibration of geobarometers for the assemblage garnet + hornblende + plagioclase + quartz. American Mineralogist, 74, 77–84.

Kohn, M.J., and Spear, F.S. (1990) Two new barometers for garnet amphibolites with applications to southeastern Vermont. American Mineralogist, 75, 89–96.

Krogh, E.J. (1980) Compatible P-T conditions for eclogites and surrounding gneisscs in the Kristiansund area, western Norway. Contributions to Mineralogy and Petrology, 75, 387–393.

Laird, J., and Albee, A.L. (1981) Pressure, temperature and time indicators in mafic schist: their application to reconstructing the polymetamorphic history of Vermont. American Journal of Science, 281, 127-175.

Leake, B.E. (1968) A catalog of analyzed calciferous and subcalciferous amphiboles together with their nomenclature and associated minerals. Special Paper. Geological Society of America.

Leake, B.E., Woolley, A.R., Arps, C.E.S., Birch W.D., Gilbert, M.C., Grice J.D., Hawthorne, F.C., Kato, A., Kisch, H.J., Krivovichev, V.G., and others (1997) Nomenclature of amphiboles: report of the Subcommittee on Amphiboles of the International Mineralogical Association, Commission on New minerals and Mineral Names. American Mineralogist, 82, 1019–1037.

Li, X.H., Zhang, C., Almeev, R.R., Zhang, X.-C., Zhao, X.-F., Wang, L.-X., Koepke, J., and Holtz F. (2019). Electron probe microanalysis of $Fe^{2+}/\Sigma Fe$ ratios in calcic and sodic-calcic amphibole and biotite using the flank method. Chemical Geology, 509, 152–162.

Mäder, U.K., and Berman, R.G. (1992) Amphibole thermobarometry, a thermodynamic approach, in Current research, Part E: Geological Survey of Canada Paper, 92-1E, 393–400.

Martin, R.F. (2007) Amphiboles in the igneous environment. Reviews in Mineralogy and Geochemistry, 67, 323–358.

Molina, J.F., Moreno, J.A., Castro, A., Rodruiguez, C., and Fershtater, G.B. (2015) Calcic amphibole thermobarometry in metamorphic and igneous rocks: new calibrations based on plagioclase/amphibole Al-Si partitioning and amphibole-liquid Mg partitioning. Lithos, 232, 286–305.

Molina, J.F., and Poli, S. (1998) Singular equilibria in paragonite blueschists, amphibolites and eclogites. Journal of Petrology, 39, 1325–1346.

Molina, J.F., and Poli, P. (2000) Carbonate stability and fluid composition in subducted oceanic crust: an experimental study on H_2O-CO_2-bearing basalts. Earth and Planetary Science Letters, 176, 295–310.

Molina, J.F., Scarrow, J.H., Montero, P., and Bea, F. (2009) High-Ti amphibole as a petrogenetic indicator of magma chemistry: evidence for mildly alkalic-hybrid melts during evolution of Variscan basic–ultrabasic magmatism of Central Iberia. Contributions to Mineralogy and Petrology, 158, 69–98.

Moore, G.M., and Carmichael, I.S.E. (1998) The hydrous phase equilibria (to 3 kbar) of an andesite and basaltic andesite from western Mexico: constraints on water content and conditions of phenocryst growth. Contributions to Mineralogy and Petrology, 130, 304–319.

Mutch, E.J.F., Blundy, J.D., Tattitch, B.C., Cooper, F.J., and Brooker, R.A. (2016) An experimental study of amphibole stability in low-pressure granitic magmas and a revised Al-in-hornblende geobarometer. Contributions to Mineralogy and Petrology, 171, 1–27.

Oberti, R., Hawthorne, F.C., Cannillo, E., and Cámara, F. (2007) Long-range order in amphiboles. Reviews in Mineralogy and Geochemistry, 67, 124–171.

Otten, M.T. (1984) The origin of brown hornblende in the Artfjillet gabbro and dolerites. Contributions to Mineralogy Petrology, 86, 189–199.

Pichavant, M., Martel, C., Bourdier, J.L., and Scaillet, B. (2002) Physical conditions, structure, and dynamics of a zoned magma chamber: Mount Peleé(Martinique, Lesser Antilles Arc). Journal of Geophysical Research, 107, 1–25.

Pietranik, A., Holtz, F., Koepke, J., and Puziewicz, J. (2009) Crystallization of quartz dioritic magmas at 2 and 1 kbar: experimental results. Mineralogy and Petrology, 97, 1–21.

Poli, S. (1993) The amphibole–eclogite transformation, an experimental study on basalt. American Journal of Science, 293, 1061–1107.

Popp, R.K., and Bryndzia, L.T. (1992) Statistical analysis of Fe^{3+}, Ti, and OH in kaersutite from alkalic igneousrocks and mafic mantle xenoliths. American Mineralogist, 77, 1250–1257,

Powell R., and Holland T.J.B. (1993) On the formulation of simple mixing models for complex phases. American Mineralogist, 7, 1174–1180.

Putirka, K.D. (2008) Thermometers and barometers for volcanic systems. Reviews in Mineralogy and Geochemistry, 69, 61–120.

Putirka, K.D. (2016) Amphibole thermometers and barometers for igneous systems, and some implications for eruption mechanisms of felsic magmas at arc volcanoes. American Mineralogist, 101, 841–858.

Ramberg, H., and De Vore, D.G.W. (1951) The distribution of Fe^{2+} and Mg in coexisting olivines and pyroxenes. Journal of Geology, 59, 193–210.

Ravna, E.J.K. (2000) Distribution of Fe^{2+} and Mg between coexisting garnet and hornblende in synthetic and natural systems: an empirical calibration of the garnet-hornblende Fe-Mg geothermometer. Lithos, 53, 265–277.

Ridolfi, F., and Renzulli, A. (2012) Calcic amphiboles in calc-alkaline and alkaline magmas: thermobarometric and chemometric empirical equations valid up to 1,130 °C and 2.2 GPa. Contributions to Mineralogy and Petrology, 163, 877–895.

Ridolfi, F., Renzulli, A., and Puerini, M. (2010) Stability and chemical equilibrium of amphibole in calc-alkaline magmas: an overview, new thermobarometric formulations and application to subduction-related volcanoes. Contributions to Mineralogy and Petrology, 160, 45–66.

Robinson, P., Spear, F.S., Schumacher, J.C., Laird, J., Klein, C., Evans, B.W., and Doolan, B.L. (1982) Phase relations of metamorphic amphiboles: natural occurrence and theory. Reviews in Mineralogy, 9B, 1–227.

Schmidt, M.W. (1992) Amphibole composition in tonalite as a function of pressure: an experimental calibration of the Al-in-hornblende barometer. Contributions to Mineralogy and Petrology, 110, 304–310.

Schumacher, J.C. (2007) Metamorphic amphiboles: composition and coexistence. Reviews in Mineralogy and Geochemistry, 67, 359–416.

Sisson, T.W., Grove, T.L., and Coleman, D.S. (1996) Hornblende gabbro sill complex at Onion Valley, California, and a mixing origin for the Sierra-Nevada batholith. Contributions to Mineralogy and Petrology, 126, 81–108.

Smithies, R.H., and Bagas, L. (1997) High-pressure amphibolite–granulite facies metamorphism in the Paleoproterozoic Rudall Complex, central Western Australia. Precambrian Research, 83, 243–265.

Spear, F.S. (1980) NaSi–CaAl exchange equilibrium between plagioclase and amphibole. An empirical model. Contributions to Mineralogy and Petrology 72, 33–41.

Spear, F.S. (1981) Amphibole-plagioclase equilibria: an empirical model for the relation albite + tremolite = edenite + 4 quartz. Contributions to Mineralogy and Petrology, 77, 355–364.

Spear, F.S. (1993) Metamorphic phase equilibria and pressure-temperature-time paths. Mineralogical Society of America Monograph.

Spear, F.S., and Kimball, C. (1984) RECAMP – a FORTRAN IV program for estimating Fe^{3+} contents in amphiboles. Computer Geoscience, 10, 317–325.

Thompson, J.B. Jr, Laird, J., and Thompson, A.B. (1982) Reactions in amphibolite, greenschist and blueschist. Journal of Petrology, 23, 1–27.

Verardi, V., and Croux, C. (2009) Robust regression in Stata. The Stata Journal, 9, 439–453.

Weaver, B.L., Tarney, J., Windley, B., and Leake, B.E. (1982) Geochemistry and petrogenesis of Archean metavolcanic amphibolites from Fiskenæsset, S.W. Greenland. Geochimica et Cosmochimica Acta, 46, 2203–2215.

Welch, M.D., Cámara, F., Della Ventura, G., and Iezzi G. (2007) Non-ambient in situ studies of amphiboles. Reviews in Mineralogy and Geochemistry, 67, 223–260.

Werts, K., Barnes, C.G., Memeti, V., Ratschbacher, B., Williams, D., and Paterson, S.R. (2020) Hornblende as a tool for assessing mineral-melt equilibrium and recognition of crystal accumulation. American Mineralogist, 105, 77–91.

Whitney, D.L., and Evans, B.W. (2010) Abbreviations for names of rock-forming minerals. American Mineralogist, 95, 185–187.

Will, T.M., and Powell, R. (1992) Activity-composition relationships in multicomponent amphiboles: an application of Darken's quadratic formalism. American Mineralogist, 77, 954–966.

Wones, D.R., and Gilbert, M.C. (1982) Amphiboles in the igneous environment. Reviews in Mineralogy, 9B, 355–390.

Yohai, V.J. (1987) High breakdown point and high efficiency robust estimates for regression. Annals of Statistics, 15, 642–656.

Zhang, J., Humphreys, M.C.S., Cooper, G.F., Davidson, J.P., and Macpherson, C.G. (2017) Magma mush chemistry at subduction zones, revealed by new melt major element inversion from calcic amphiboles. American Mineralogist, 102, 1353–1367.

Figure captions

Fig. 1. Importance of accuracy for a meaningful precision. A) Experimental temperatures versus temperatures calculated with the amphibole-plagioclase NaSi–CaAl exchange thermometer from Holland and Blundy (1994). Temperature estimates for a thermometer with a perfect accuracy cluster along the one-to-one line. B) Relationships of residuals versus amphibole Mg occupancy for the same thermometer. Data source: Conrad et al. (1988), Schmidt (1992), Moore and Carmichael (1998), Pichavant et al. (2002) and Pietranik et al. (2009). See text for discussion.

Fig. 2. Composition of amphibole coexisting with plagioclase from the experimental data sets. A) Al^{IV} vs. Na^{A} + K. B) Al^{IV} vs. Na^{M4}. C) Al^{IV} vs. Ti. D) Al^{IV} vs. $Mg/(Mg+Fe^{2+})$. Abbreviations: CDS2, Calibration Data Set 2; TDS2, Test Data Set 2; OUT, outliers.

Fig. 3. Composition of plagioclase coexisting with amphibole from the experimental data sets. A) Histogram of anorthite content in plagioclase. B) Composition of plagioclase in the Ab-An-Or ternary. Abbreviations: CDS2, Calibration Data Set 2; TDS2, Test Data Set 2; OUT, outliers.

Fig. 4. Diagnostic plots of robust standardized residuals versus Mahalanobis distance for the expressions derived in this work using MM-estimators reported in Table 5. Thermodynamic models: A1, calculated with CDS1 using $\Delta G_{pl}^{ex}(EG90)$; A2, calculated with CDS2 using $\Delta G_{pl}^{ex}(EG90)$; B1, calculated with CDS1 using $\Delta G_{pl}^{ex}(HP92)$; B2, calculated with CDS2 using $\Delta G_{pl}^{ex}(HP92)$.

Fig. 5. Experimental temperatures versus temperatures calculated with the new calibrations of the amphibole-plagioclase NaSi–CaAl exchange thermometer derived in this work. A) Expression A1. B) Expression B1. C) Expression A2. D) Expression B2. Abbreviations: CDS1, Calibration Data Set 1; CDS2, Calibration Data Set 2; TDS2, Test Data Set 2; FDS, Full Data Set; OUT, outliers.

Fig. 6. Relationships of residuals versus amphibole Na^{M4} occupancy for the new amphibole-plagioclase NaSi–CaAl exchange thermometers. A) Expressions A1 and B1. B) Expressions A2 and B2.

Abbreviations: CDS1, Calibration Data Set 1; CDS2, Calibration Data Set 2; TDS2, Test Data Set 2; FDS, Full Data Set; OUT, outliers.

Fig. 7. Relationships of residuals versus anorthite content of plagioclase for the new amphibole-plagioclase NaSi–CaAl exchange thermometers. A) Expressions A1 and B1. B) Expressions A2 and B2. Abbreviations: CDS1, Calibration Data Set 1; CDS2, Calibration Data Set 2; TDS2, Test Data Set 2; FDS, Full Data Set; OUT, outliers.

Fig. 8. Experimental temperatures versus temperatures calculated with amphibole-plagioclase and amphibole-only thermometers from the literature. A) Amphibole-plagioclase NaSi–CaAl exchange thermometer from Holland and Blundy (1994): expression B (Exp. B-H&B94). B) Amphibole-only thermometer from Ridolfi and Renzulli (2012): expression 2 (Exp. 2-RR12). C) Amphibole-only thermometer from Putirka (2016): expression 5 (Exp. 5-P16). D) Amphibole-only thermometer from Putirka (2016): expression 6 (Exp. 6-P16). Abbreviations: CDS2, Calibration Data Set 2; TDS2, Test Data Set 2; FDS, Full Data Set; OUT, outliers; CTR, Calibration Temperature Range; FTR, Full Temperature Range.

Fig. 9. Relationships of residuals versus amphibole and plagioclase compositions for the amphibole-plagioclase NaSi–CaAl exchange thermometer from Holland and Blundy (1994): expression B (Exp. B-H&B94). Abbreviations: CDS2, Calibration Data Set 2; TDS2, Test Data Set 2; FDS, Full Data Set; OUT, outliers; CTR, Calibration Temperature Range; FTR, Full Temperature Range.

Fig. 10. Relationships of residuals versus amphibole composition. A) Amphibole-only thermometer from Ridolfi and Renzulli (2012): expression 2 (Exp. 2-RR12). B) Amphibole-only thermometer from Putirka (2016): expression 5 (Exp. 5-P16). C) Amphibole-only thermometer from Putirka (2016): expression 6 (Exp. 6-P16). Abbreviations: CDS2, Calibration Data Set 2; TDS2, Test Data Set 2; FDS, Full Data Set; OUT, outliers; CTR, Calibration Temperature Range; FTR, Full Temperature Range.

Fig. 11. Application of the new calibrated expressions to amphibole-plagioclase pairs from igneous and high-grade metamorphic rocks. Estimated temperatures versus discrepancies between average temperature estimates obtained by the new amphibole-plagioclase NaSi–CaAl exchange thermometers and the calibration from Holland and Blundy (1994) (expression B, Exp. B-H&B94). A) Expression A1. B) Expression A2. C) Expression B2. Uncertainty bands reported at 1s (±50ºC) and 2s (±100ºC) levels (see text for explanation).

Fig. 12. Application of the new calibrated expressions to amphibole-plagioclase pairs from igneous and high-grade metamorphic rocks. Amphibole composition versus discrepancies between average temperature estimates obtained by the new amphibole-plagioclase NaSi–CaAl exchange thermometers and the calibration from Holland and Blundy (1994) (expression B, Exp. B-H&B94). A) Expression A1. B) Expression A2. C) Expression B2. Uncertainty bands reported at 1s (±50ºC) and 2s (±100ºC) levels (see text for explanation).

Fig. 13. Application of the new calibrated expressions to amphibole-plagioclase pairs from igneous rocks. Estimated temperatures and amphibole composition versus discrepancies between average temperature estimates obtained by the new amphibole-plagioclase NaSi–CaAl exchange thermometers and the amphibole-only thermometers from Ridolfi and Renzulli (2012) (expression 2, Exp. 2) and Putirka (2016) (expressions 5, Exp. 5, and 6, Exp. 6). A) Expression A1. B) Expression A2. C) Expression B2. Uncertainty bands reported at 1s (±50ºC) and 2s (±100ºC) levels (see text for explanation).

DOI: https://doi.org/10.2138/am-2021-7400. http://www.minsocam.org/

Electronic supplementary material

Appendix A. Summary of the experimental data sets

Appendix B. Supplementary Figures and Tables

Appendix C. Procedure for outlier detection

Appendix D. Amphibole-plagioclase thermobarometry

Appendix E. Selected amphibole-plagioclase pairs from igneous and high-grade metamorphic rocks

TABLES

Table 1. Cation fraction in sites and molar fraction of phase components

Plagioclase

Phases component	*Molar fraction*
Albite	$p_{ab} = Na/(Na + K + Ca)$
Anorthite	$p_{an} = Ca/(Na + K + Ca)$
Orthoclase	$p_{or} = K/(Na + K + Ca)$

Amphibole *(cations normalized to 23O)*

Cation	*Site*	*Atomic fraction*
Si	*T1*	$X_{Si}^{T1} = (Si - 4)/4$
Al	*T1*	$X_{Al}^{T1} = (8 - Si)/4$
Ti	*M2*	$X_{Ti}^{M2} = Ti/2$
Al	*M2*	$X_{Al}^{M2} = (Si + Al - 8)/2$
Cr	*M2*	$X_{Cr}^{M2} = Cr/2$
Fe^{3+}	*M2*	$X_{Fe^{3+}}^{M2} = Fe^{3+}/2$
Fe^{2+}	*M2*	$X_{Fe^{2+}}^{M2} = r\,(10 - Si - Ti - Al - Cr - Fe^{3+})/2$ where $r = Fe^{2+}/(Fe^{2+} + Mg)$
Mg	*M2*	$X_{Mg}^{M2} = (1 - r)\,(10 - Si - Ti - Al - Cr - Fe^{3+})/2$
Mg	*M4*	$X_{Mg}^{M4} = (1 - r)\,(\Sigma - 13 - Ca - Mn - Na - K)/2$ where $\Sigma = Si + Ti + Al + Cr + Fe + Mn + Mg + Ca + Na + K$
Mn	*M4*	$X_{Mn}^{M4} = Mn/2$
Na	*M4*	$X_{Na}^{M4} = (Na + K + 15 - \Sigma)/2$
Na	*A*	$X_{Na}^{A} = \Sigma - K - 15$
K	*A*	$X_{K}^{A} = K$

Phase component	*Order*	*T1*	*T2*	*M2*	*M13*	*M4*	*A*	*Molar fraction*
Glaucophane	1	Si_4	Si_4	Al_2	Mg_3	Na_2	□	$p_1 = X_{Na}^{M4}$
Aluminotschermakite	2	Si_2Al_2	Si_4	Al_2	Mg_3	Ca_2	□	$p_2 = X_{Al}^{M2} - (X_{Na}^{M4} + 0.5\,X_{Na}^{A} + 0.5\,X_{K}^{A})$
Ti-tschermakite	3	Al_4	Si_4	Ti_2	Mg_3	Ca_2	□	$p_3 = X_{Ti}^{M2}$
Ferritschermakite	4	Si_2Al_2	Si_4	Fe_2^{3+}	Mg_3	Ca_2	□	$p_4 = X_{Fe^{3+}}^{M2}$
Pargasite	5	Si_2Al_2	Si_4	$AlMg$	Mg_3	Ca_2	Na	$p_5 = X_{Na}^{A}$
K-pargasite	6	Si_2Al_2	Si_4	$AlMg$	Mg_3	Ca_2	K	$p_6 = X_{K}^{A}$
Cummingtonite	7	Si_4	Si_4	Mg_2	Mg_3	Mg_2	□	$p_7 = X_{Mg}^{M4}$
Ferro-actinolite	8	Si_4	Si_4	Fe_2^{2+}	Fe_3^{2+}	Ca_2	□	$p_8 = X_{Fe^{2+}}^{M2}$
Tremolite	9	Si_4	Si_4	Mg_2	Mg_3	Ca_2	□	$p_9 = 1 - (p_1 + p_2 + p_3 + p_4 + p_5 + p_6 + p_7 + p_8 + p_{10} + p_{11})$
Cr-tschermakite	10	Si_2Al_2	Si_4	Cr_2^{3+}	Mg_3	Ca_2	□	$p_{10} = X_{Cr}^{M2}$
Manganocummingtonite	11	Si_4	Si_4	Mg_2	Mg_3	Mn_2	□	$p_{11} = X_{Mn}^{M4}$

Abbreviations of amphibole end-member components: glaucophane (gln), aluminotschermakite (ts), Ti-tschermakite (tts), ferritschermakite (fts), pargasite (prg), K-pargasite (kprg), cummingtonite (cum), ferro-actinolite (fact), tremolite (tr), Cr-tschermakite (crts) and manganocummingtonite (mncum).

Table 2. Amphibole site allocations

Site	Multiplicity	Cations
T1	4	Si^{4+}, Al^{3+}
T2	4	Si^{4+}
M2	2	Ti^{4+}, Al^{3+}, Cr^{3+}, Fe^{3+}, Fe^{2+}, Mg^{2+}, Mn^{2+}
M13	3	Fe^{2+}, Mg^{2+}, Mn^{2+}
M4	2	Fe^{2+}, Mg^{2+}, Mn^{2+}, Ca^{2+}, Na^{+}
A	1	Na^{+}, K^{+}, □

782

Table 3. Amphibole mixing parameters for $\Delta G_{amp}^{ex} = RTln\gamma_{gln} - RTln\gamma_{ts}$

Parameter	*Linear combination of interaction mixing parameters*
W_0	$W_{gln\,tr} - W_{ts\,tr}$
W_1	$W_{ts\,tr} - W_{gln\,tr} - W_{gln\,ts}$
W_2	$W_{ts\,tr} - W_{gln\,tr} + W_{gln\,ts}$
W_3	$W_{ts\,tr} - W_{gln\,tr} + W_{gln\,tts} - W_{ts\,tts}$
W_4	$W_{ts\,tr} - W_{gln\,tr} + W_{gln\,fts} - W_{ts\,fts}$
W_5	$W_{ts\,tr} - W_{gln\,tr} + W_{gln\,prg} - W_{ts\,prg}$
W_6	$W_{ts\,tr} - W_{gln\,tr} + W_{gln\,kprg} - W_{ts\,kprg}$
W_7	$W_{ts\,tr} - W_{gln\,tr} + W_{gln\,cum} - W_{ts\,cum}$
W_8	$W_{ts\,tr} - W_{gln\,tr} + W_{gln\,fact} - W_{ts\,fact}$

Table 4. Excess Gibbs free energy of reaction for plagioclase

Ternary feldspar solution model of Elkins and Grove (1990). Units: J, K and bar

$$\Delta G_{pl}^{ex}(EG90) = 2W_{anab}p_{ab}^2 - 2W_{aban}p_{an}^2 +$$
$$2(W_{an\,or} - W_{ab\,or})p_{or}^2 + 4(W_{ab\,an} - W_{an\,ab})p_{an}p_{ab} +$$
$$(3W_{or\,an} - W_{ab\,an} - W_{ab\,or} - W_{an\,ab} - W_{an\,or} - W_{or\,ab} - 2W_{or\,ab\,an})p_{an}p_{or} +$$
$$(W_{ab\,an} + W_{ab\,or} + W_{an\,ab} + W_{an\,or} + W_{or\,an} - 3W_{or\,ab} + 2W_{or\,ab\,an})p_{or}p_{ab}$$

$$W_{an\,ab} = 0$$
$$W_{ab\,an} = 7924$$
$$W_{or\,an} = 40317$$
$$W_{an\,or} = 38974 - 0.1037P$$
$$W_{ab\,or} = 18810 - 10.3T + 0.4602P$$
$$W_{or\,ab} = 27320 - 10.3T + 0.3264P$$
$$W_{or\,ab\,an} = 12545 - 1.095P$$

DQF approach for plagioclase activity-composition relations of Holland and Powell (1992). Units: J and K

$I\bar{1}$ structure ($p_{an} > X_b$): $\Delta G_{pl}^{ex}(HP92) = 2W_{I\bar{1}}[(1 - p_{an})^2 - (1 - p_{ab})^2] + 2\Delta W X_b^2$

$C\bar{1}$ structure ($p_{an} < X_b$): $\Delta G_{pl}^{ex}(HP92) = 2W_{C\bar{1}}[(1 - p_{an})^2 - (1 - p_{ab})^2] + 2\Delta W(1 - X_b)^2$

$$X_b = 0.12 + 0.00038T$$

$$W_{I\bar{1}} = 10000$$

$$W_{C\bar{1}} = 1000$$

$$\Delta W = W_{I\bar{1}} - W_{C\bar{1}}$$

Table 5. Fitted thermodynamic parameters for reaction *R1* and for $\Delta G^{ex}_{amp} = RTln\gamma_{gln} - RTln\gamma_{ts}$. Modeled expression: $-\left(RTlnK^{id} + \Delta G^{ex}_{pl}\right) = A - TB + PC + \sum_{i=1}^{8}\{p_i W_i^H - p_i T W_i^S + p_i P W_i^V\}$. Parameters retrieved using MM-estimators. Units: J and J/K

Expression	*A1*	*B1*	*A2*	*B2*
Plagioclase mixing model[1]	$\Delta G^{ex}_{pl}(EG90)$	$\Delta G^{ex}_{pl}(HP92)$	$\Delta G^{ex}_{pl}(EG90)$	$\Delta G^{ex}_{pl}(HP92)$
Calibration data set[2]	*CDS1*	*CDS1*	*CDS2*	*CDS2*
Observations	196	196	92	92
Scale parameter	6361	6348	4475	4634
Thermodynamic parameters[3]				
A	(1.36±0.20) 10^5 t = 6.8	(1.40±0.20) 10^5 t = 7.0	(1.477±0.079) 10^5 t = 19	(1.48±0.12) 10^5 t = 12
B	90±19 t = 4.7	91±20 t = 4.6	94±11 t = 8.5	94±16 t = 5.9
C	0	0	0	0
W_2^H	(-2.80±0.54) 10^4 t = -5.2	(-3.02±0.50) 10^4 t = -6.0	(-3.77±0.63) 10^4 t = -6.0	(-4.01±0.87) 10^4 t = -4.6
W_5^H	(7.31±0.77) 10^4 t = 9.5	(7.08±0.77) 10^4 t = 9.2	(6.96±1.01) 10^4 t = 6.9	(7.04±1.11) 10^4 t = 6.3
W_7^S	101±27 t = 3.7	109±26 t = 4.2	132±25 t = 5.3	149±36 t = 4.1
W_8^S	72±17 t = 4.2	70±15 t =4.7	96±16 t = 6.0	93±12 t = 7.8

Notes: 1: $\Delta G^{ex}_{pl}(EG90)$, ternary feldspar solution model of Elkins and Grove (1990); $\Delta G^{ex}_{pl}(HP92)$, DQF approach for plagioclase activity-composition relations of Holland and Powell (1992). 2: CDS1, Calibration Data Set 1, for expressions A1 and B1 (i.e., full data set excluding 7 outliers); CDS2, Calibration Data Set 2, for expressions A2 and B2. 3: All selected thermodynamic parameters with $P(>|t|) = 0$, i.e., they are statistically significant.

This is the peer-reviewed, final accepted version for American Mineralogist, published by the Mineralogical Society of America.
The published version is subject to change. Cite as Authors (Year) Title. American Mineralogist, in press.
DOI: https://doi.org/10.2138/am-2021-7400. http://www.minsocam.org/

FIGURES

Figure 1

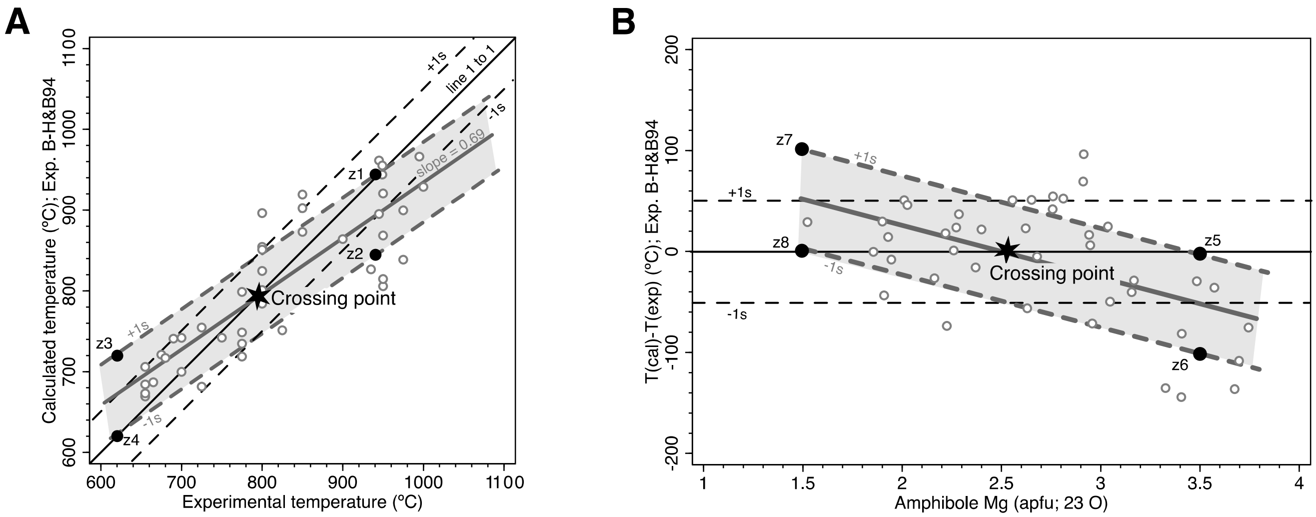

Figure 2

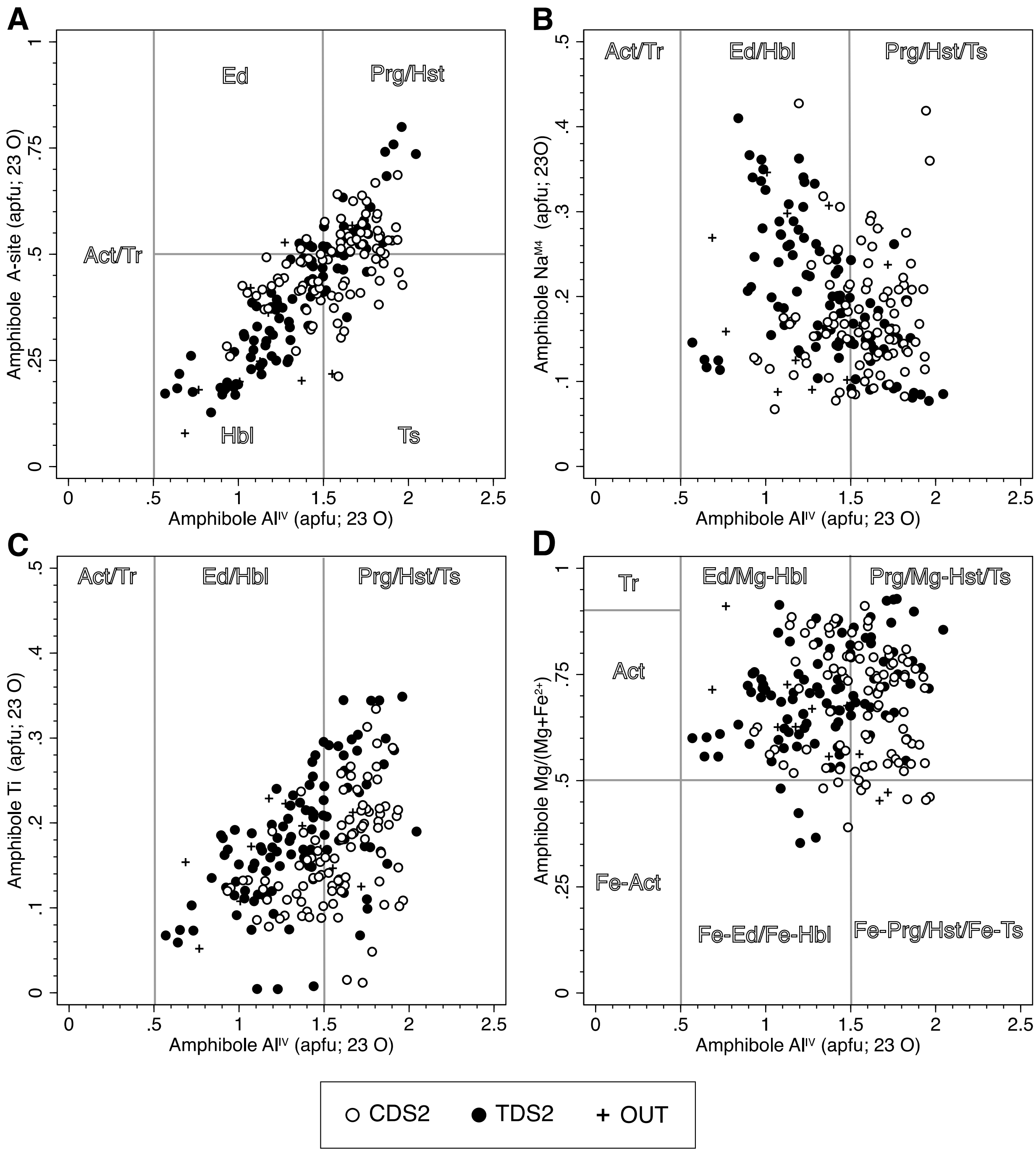

796

797

Figure 3

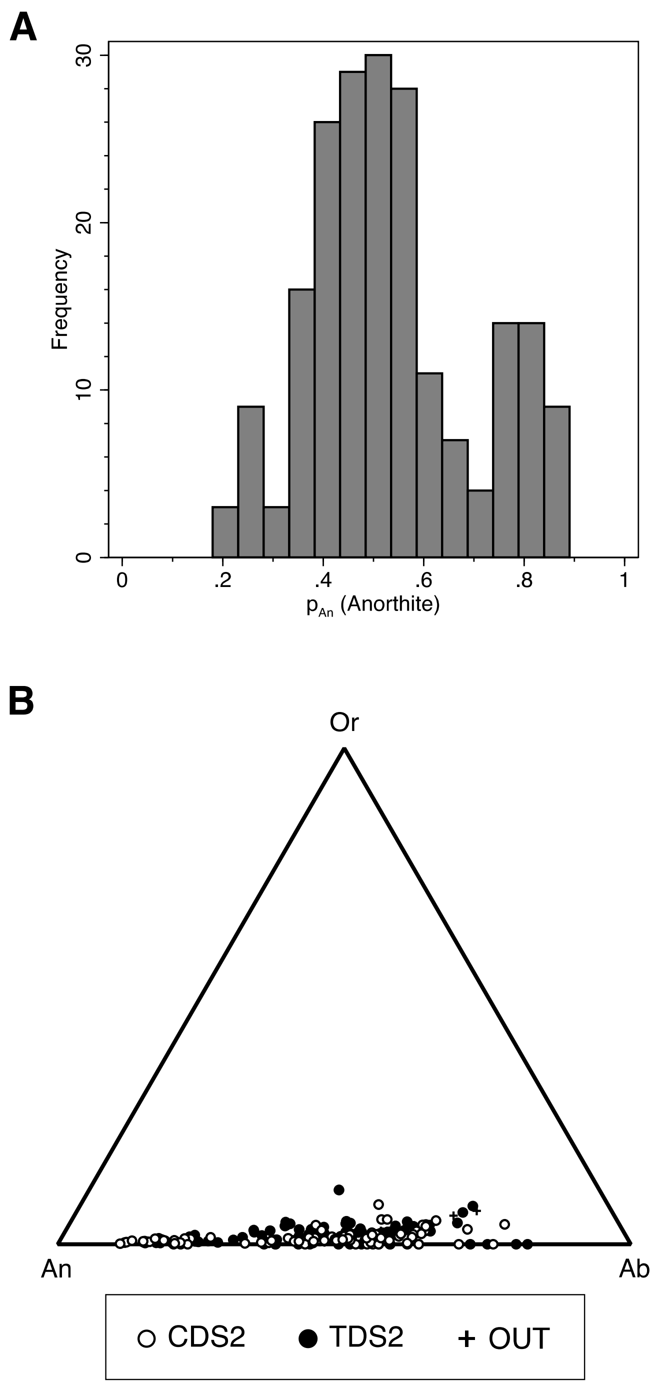
A
Frequency
0
10
20
30
0
.2
.4
.6
.8
1
p An (Anorthite)
B
Or
An
Ab
CDS2
TDS2
OUT

This is the peer-reviewed, final accepted version for American Mineralogist, published by the Mineralogical Society of America.
The published version is subject to change. Cite as Authors (Year) Title. American Mineralogist, in press.
DOI: https://doi.org/10.2138/am-2021-7400. http://www.minsocam.org/

Figure 4

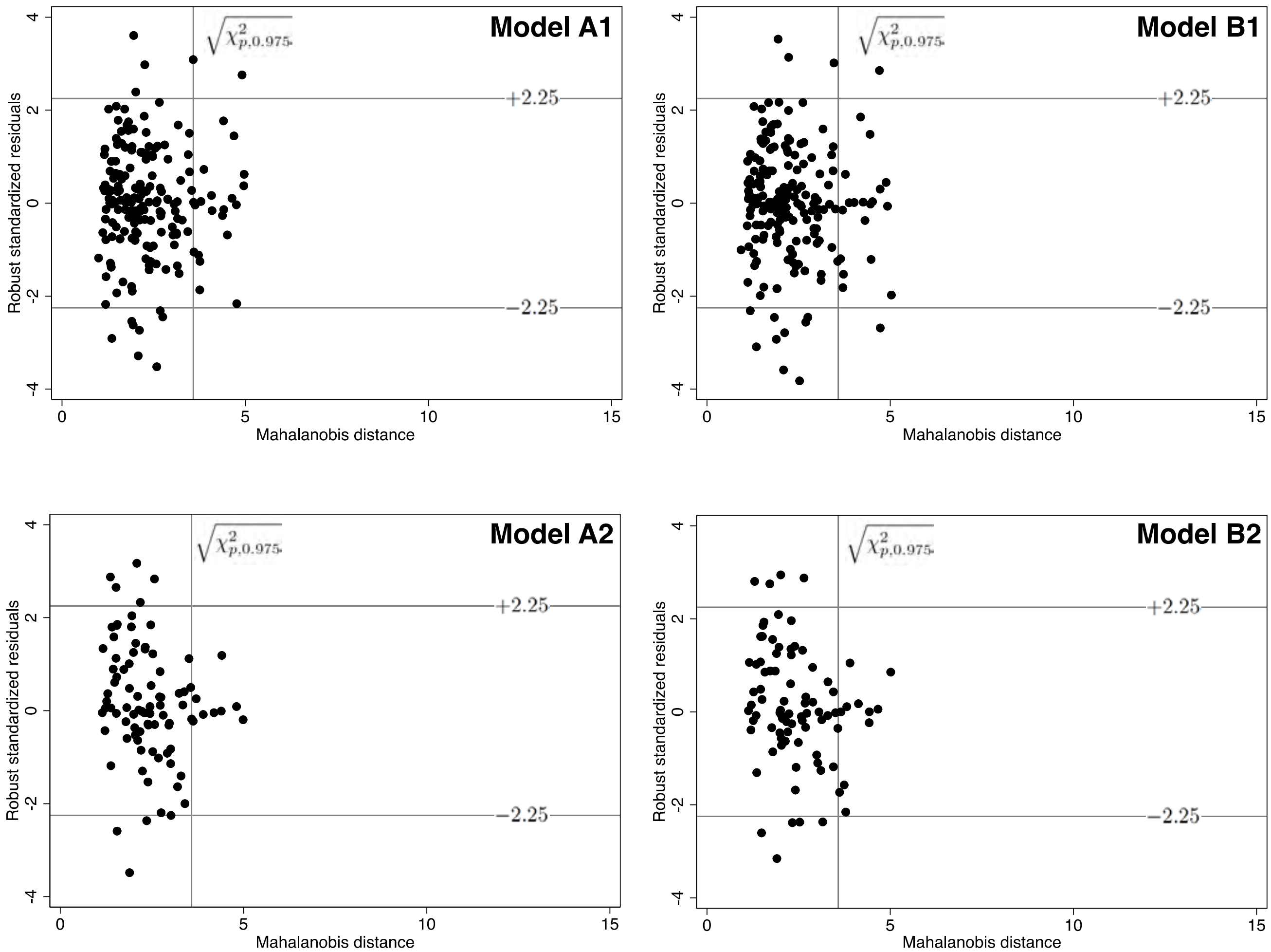

Figure 5

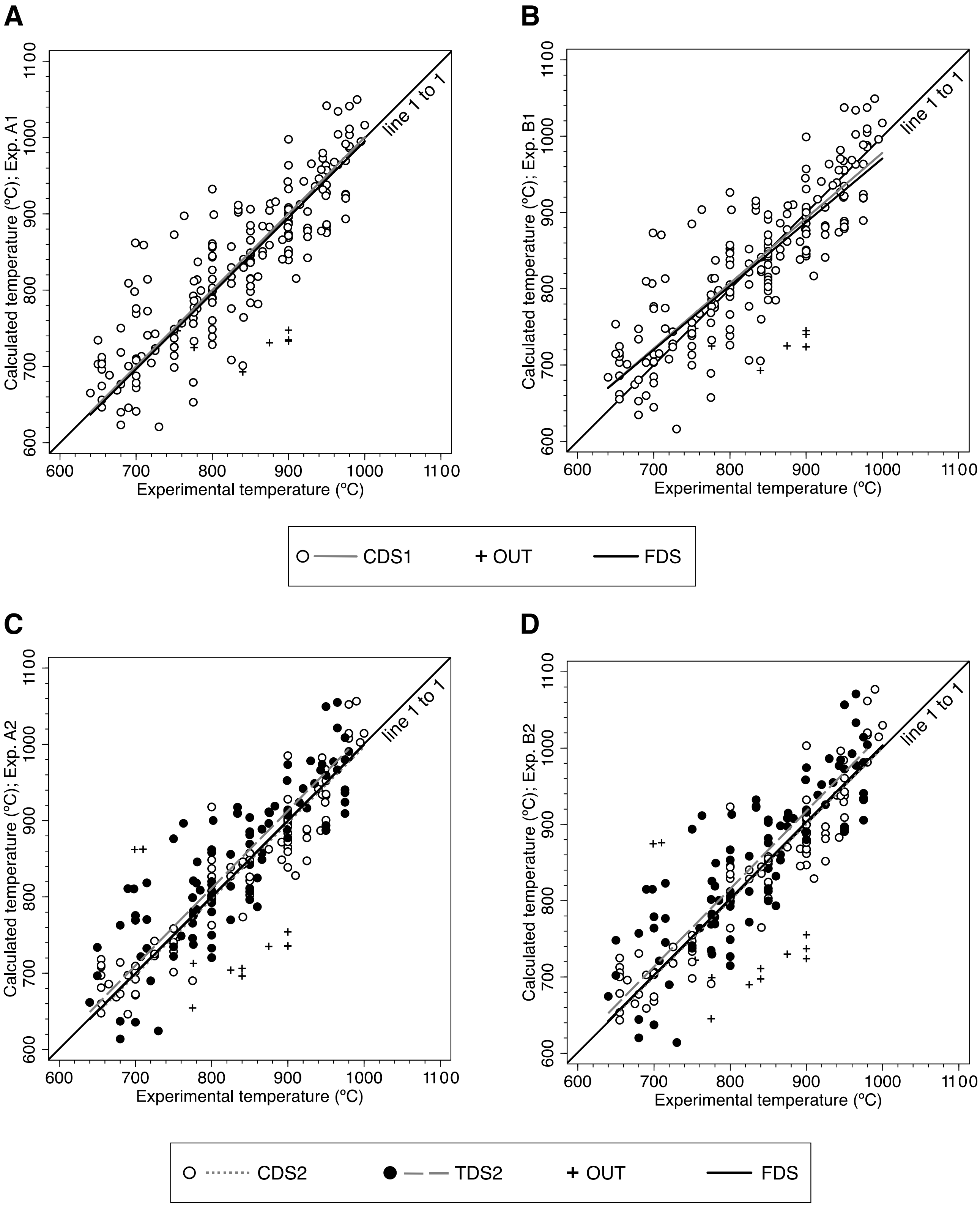
A
B
C
D
Calculated temperature (ºC); Exp. A1
Calculated temperature (ºC); Exp. B1
Calculated temperature (ºC); Exp. A2
Calculated temperature (ºC); Exp. B2
Experimental temperature (ºC)
600
700
800
900
1000
1100
line 1 to 1
CDS1
+ OUT
FDS
CDS2
TDS2
+ OUT
FDS

DOI: https://doi.org/10.2138/am-2021-7400. http://www.minsocam.org/

Figure 6

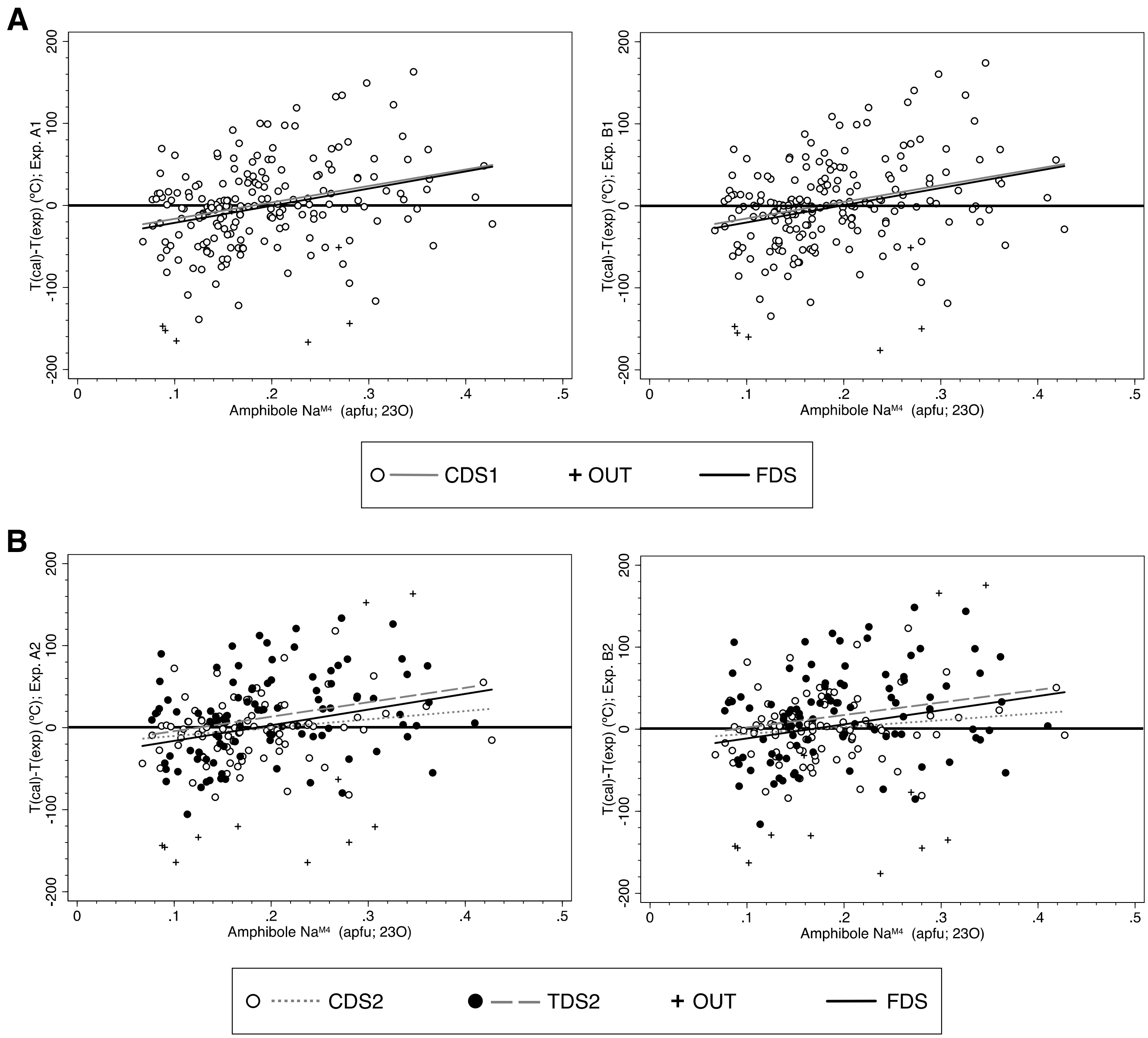

Figure 7

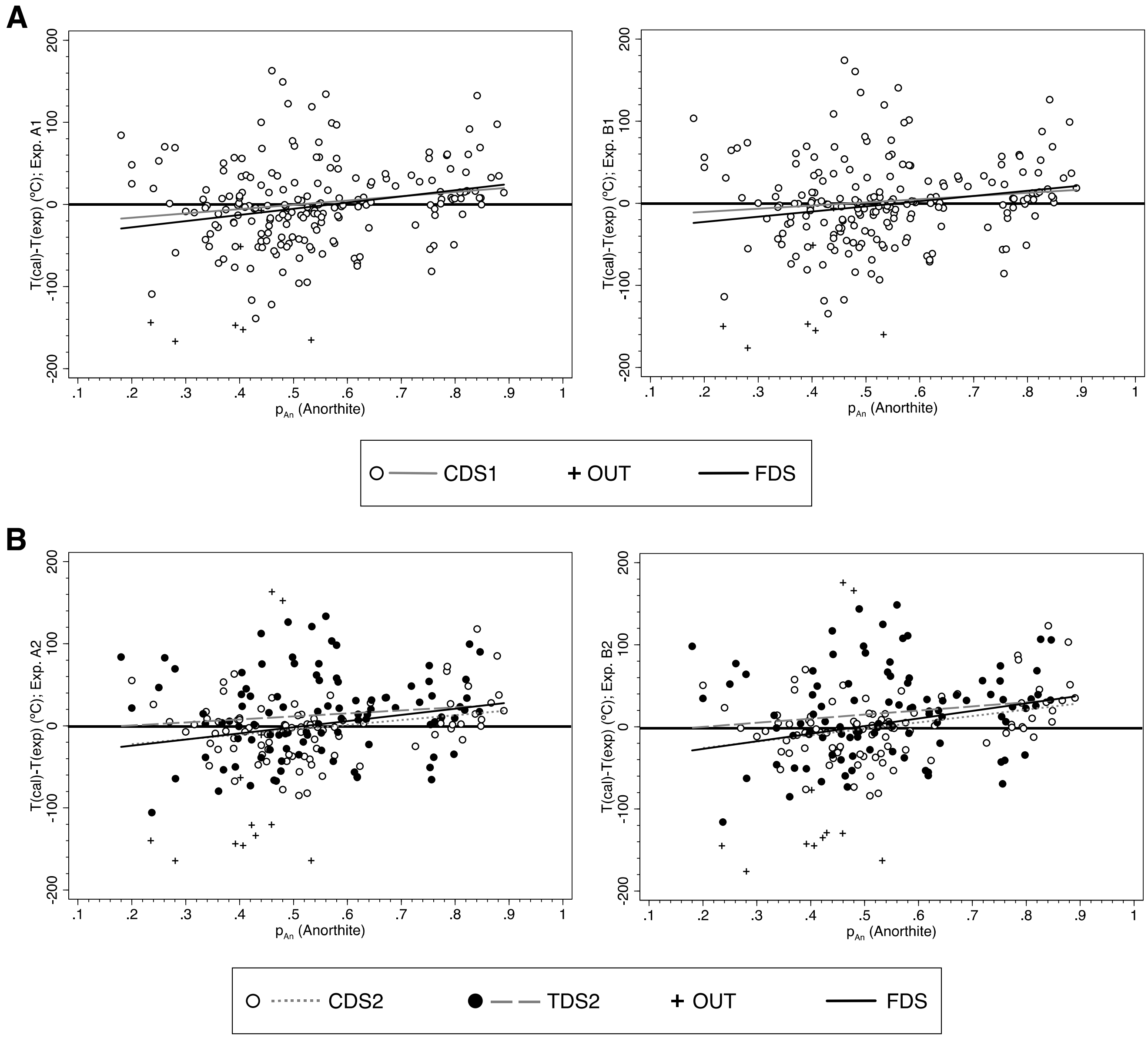
A
T(cal)-T(exp) (°C); Exp. A1
T(cal)-T(exp) (°C); Exp. B1
p_{An} (Anorthite)
CDS1
OUT
FDS
B
T(cal)-T(exp) (°C); Exp. A2
T(cal)-T(exp) (°C); Exp. B2
p_{An} (Anorthite)
CDS2
TDS2
OUT
FDS

This is the peer-reviewed, final accepted version for American Mineralogist, published by the Mineralogical Society of America.
The published version is subject to change. Cite as Authors (Year) Title. American Mineralogist, in press.
DOI: https://doi.org/10.2138/am-2021-7400. http://www.minsocam.org/

Figure 8

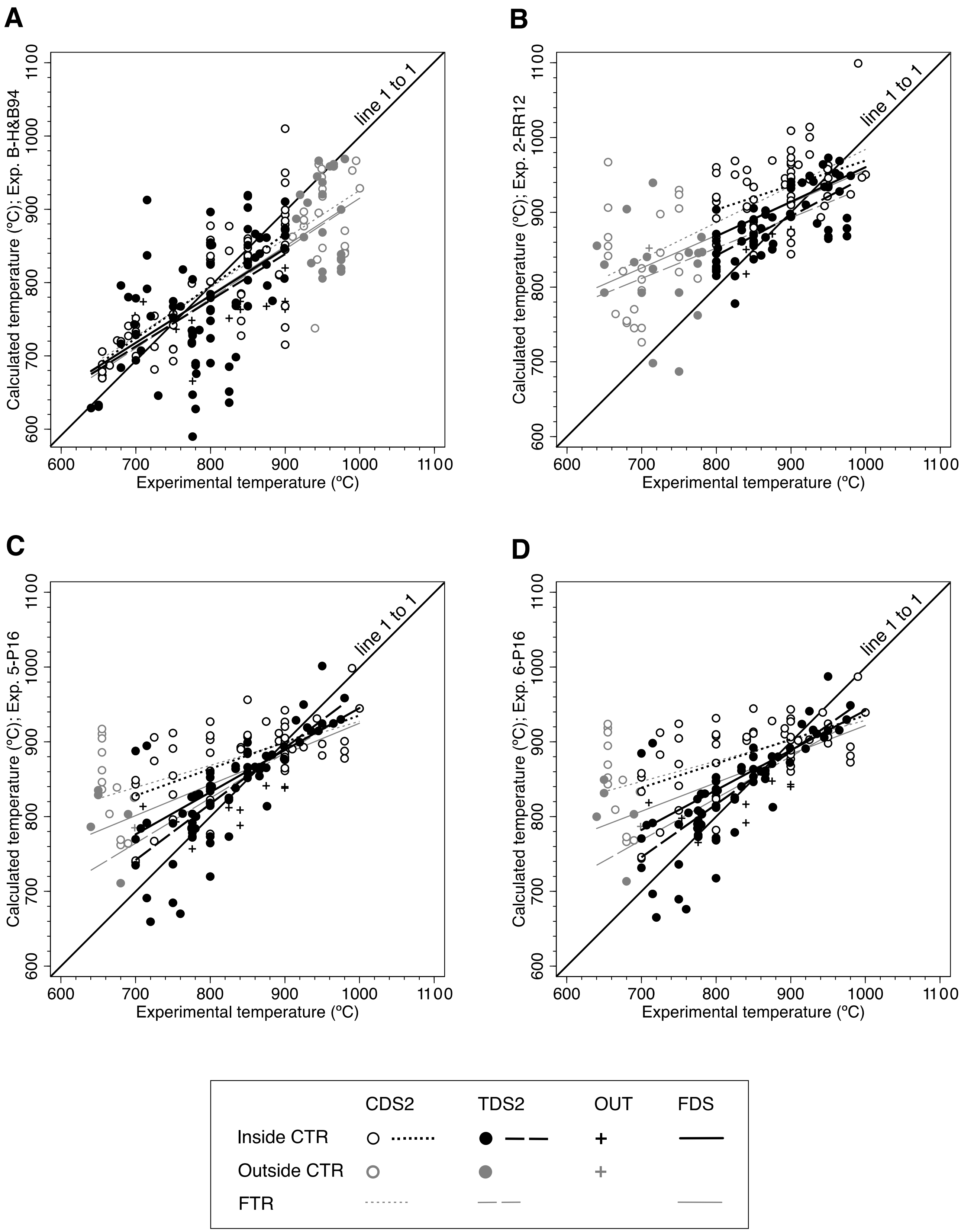

811

Figure 9

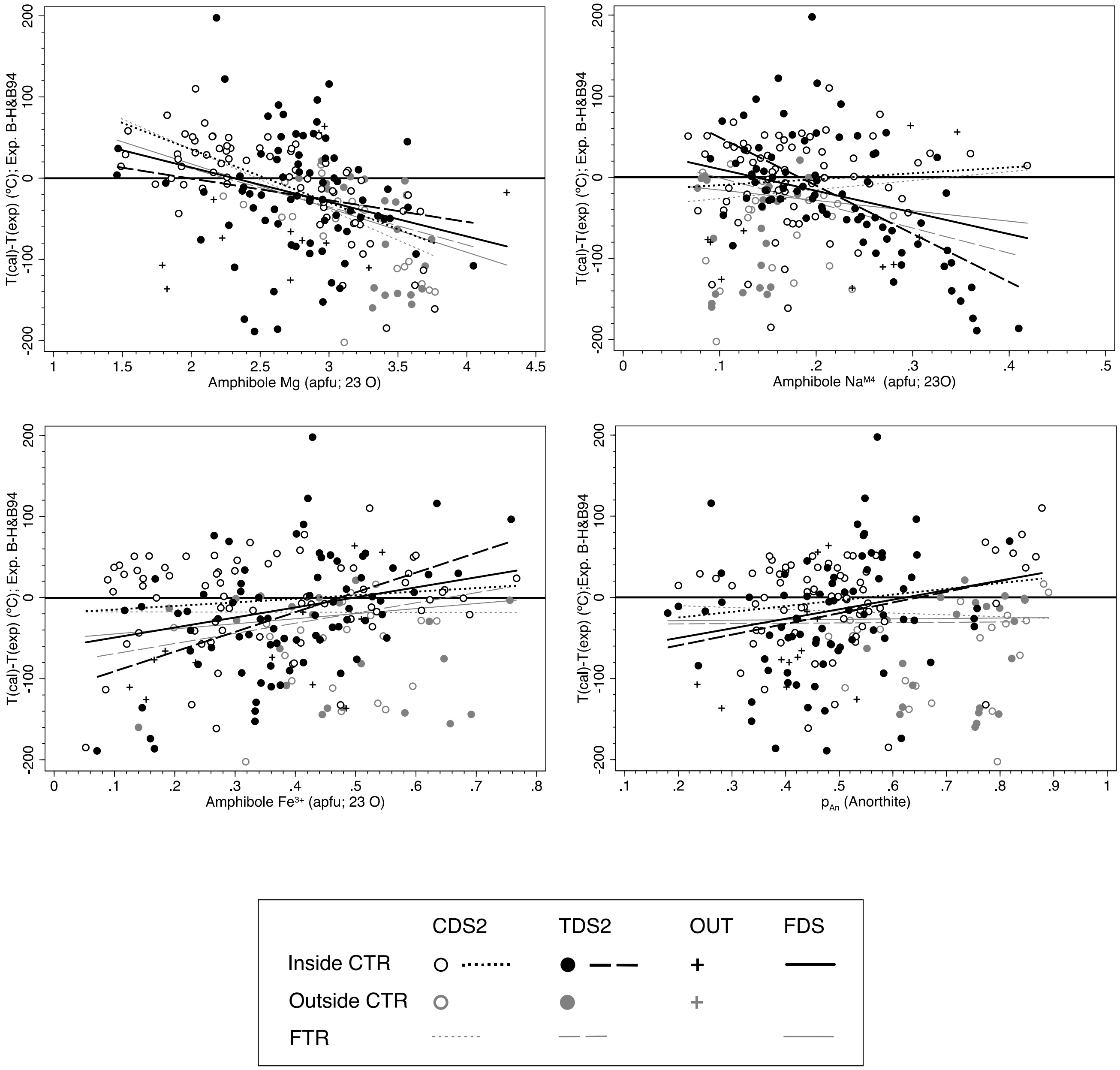
T(cal)-T(exp) (ºC); Exp. B-H&B94
Amphibole Mg (apfu; 23 O)
Amphibole Na^M4 (apfu; 23O)
Amphibole Fe³⁺ (apfu; 23 O)
T(cal)-T(exp) (ºC);Exp. B-H&B94
p_An (Anorthite)
CDS2
TDS2
OUT
FDS
Inside CTR
Outside CTR
FTR

Figure 10

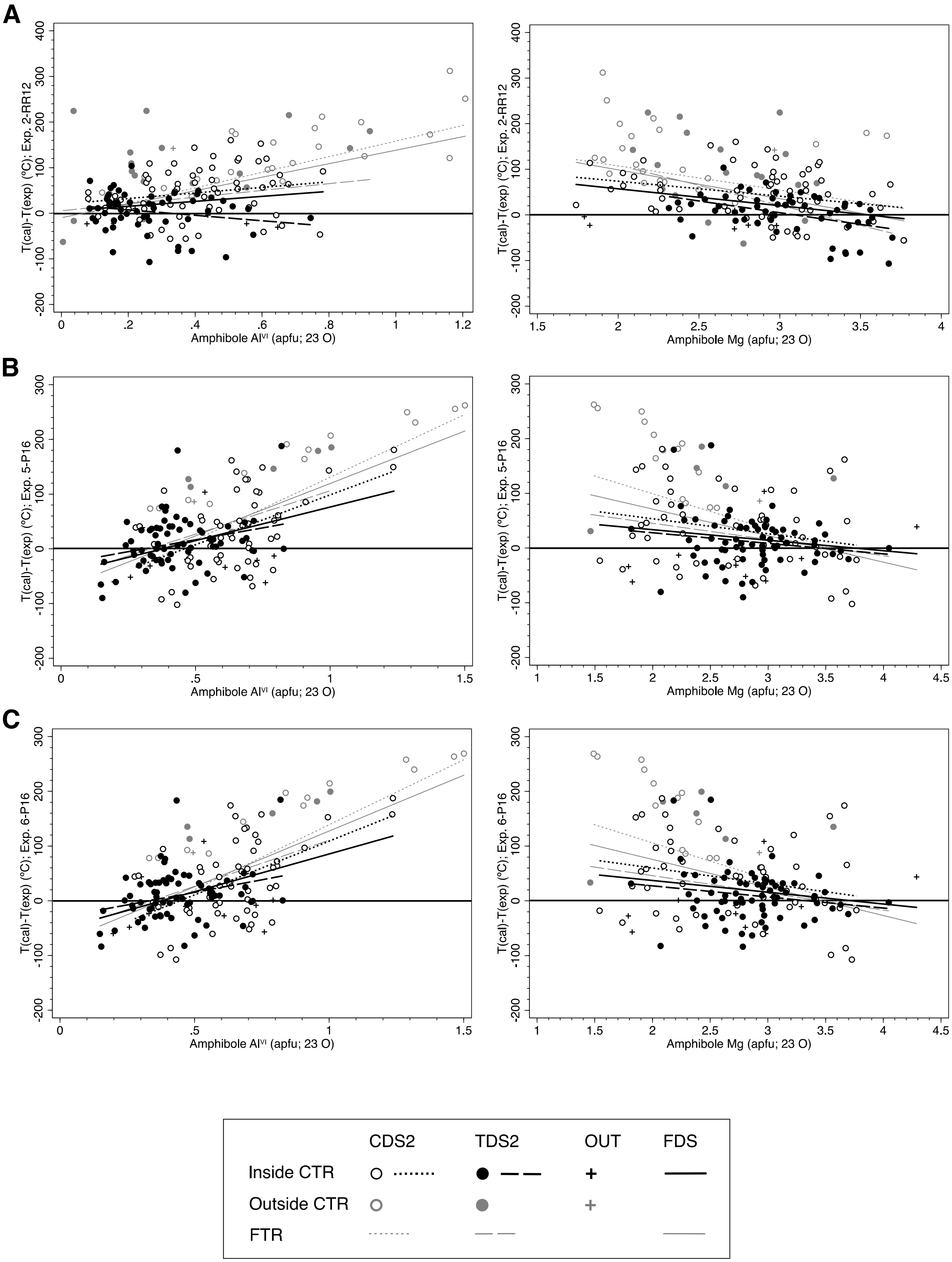
A
B
C
T(cal)-T(exp) (°C); Exp. 2-RR12
T(cal)-T(exp) (°C); Exp. 5-P16
T(cal)-T(exp) (°C); Exp. 6-P16
Amphibole Al^{VI} (apfu; 23 O)
Amphibole Mg (apfu; 23 O)
CDS2
TDS2
OUT
FDS
Inside CTR
Outside CTR
FTR

This is the peer-reviewed, final accepted version for American Mineralogist, published by the Mineralogical Society of America.
The published version is subject to change. Cite as Authors (Year) Title. American Mineralogist, in press.
DOI: https://doi.org/10.2138/am-2021-7400. http://www.minsocam.org/

Figure 11

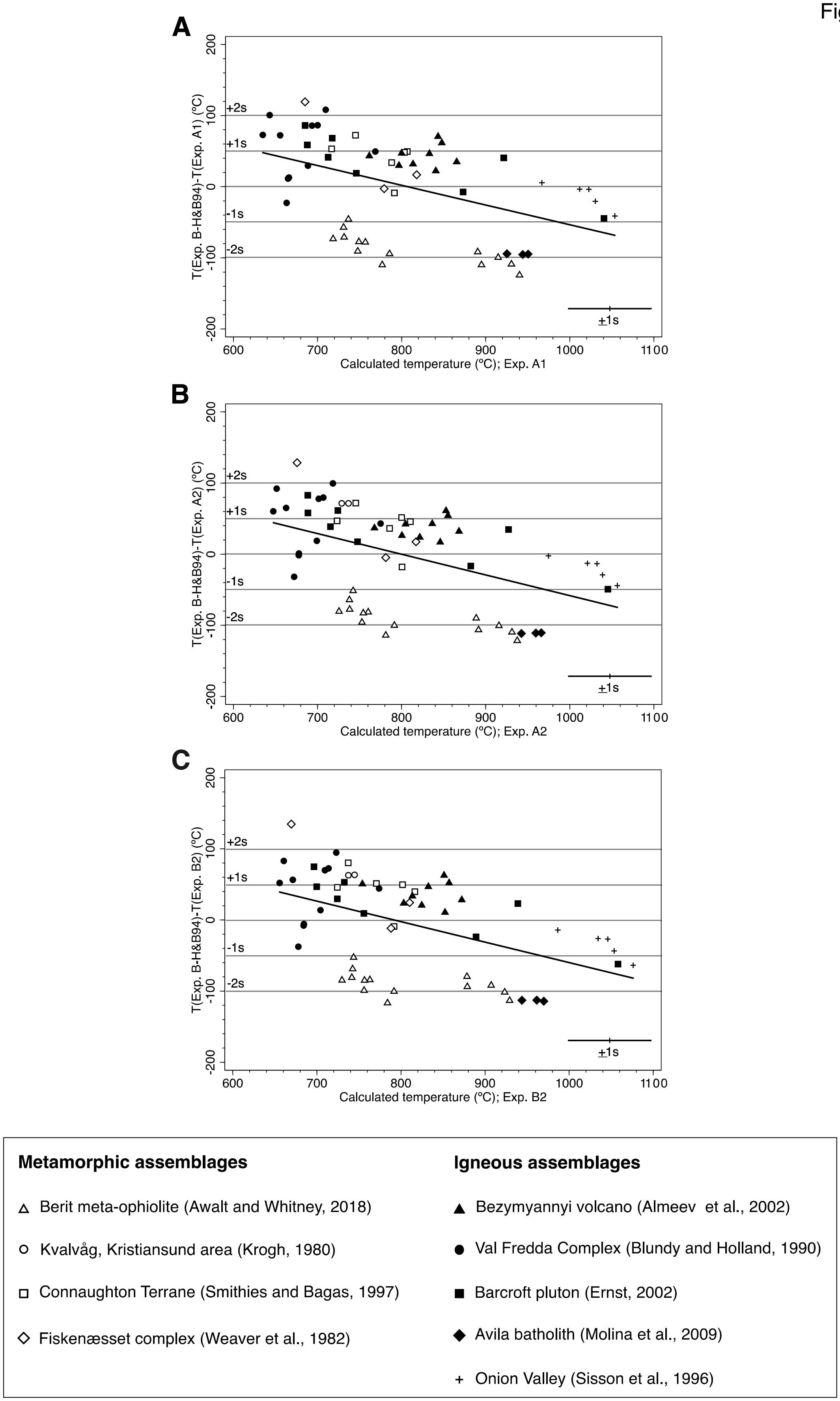

816

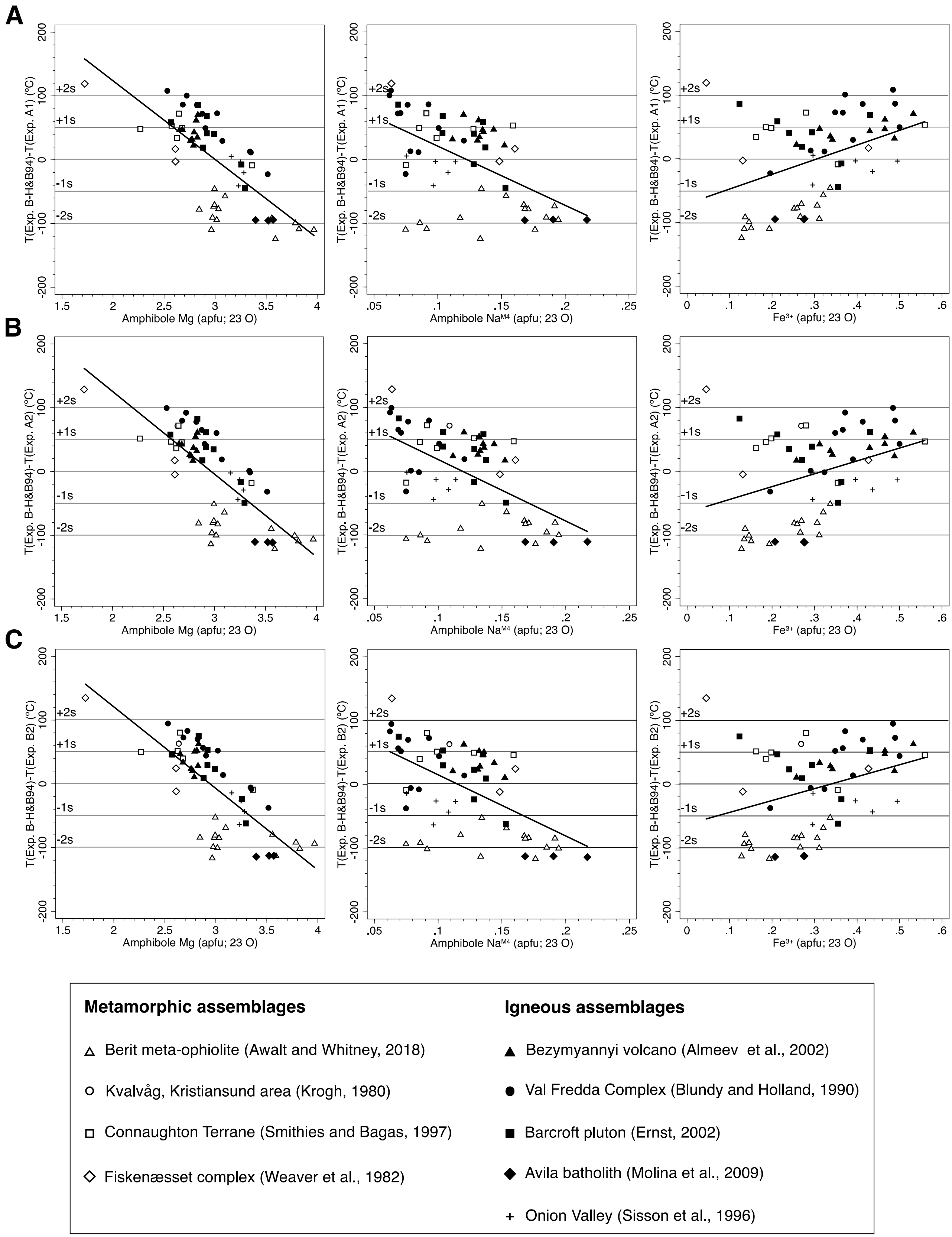

817

Figure 12

Figure 13

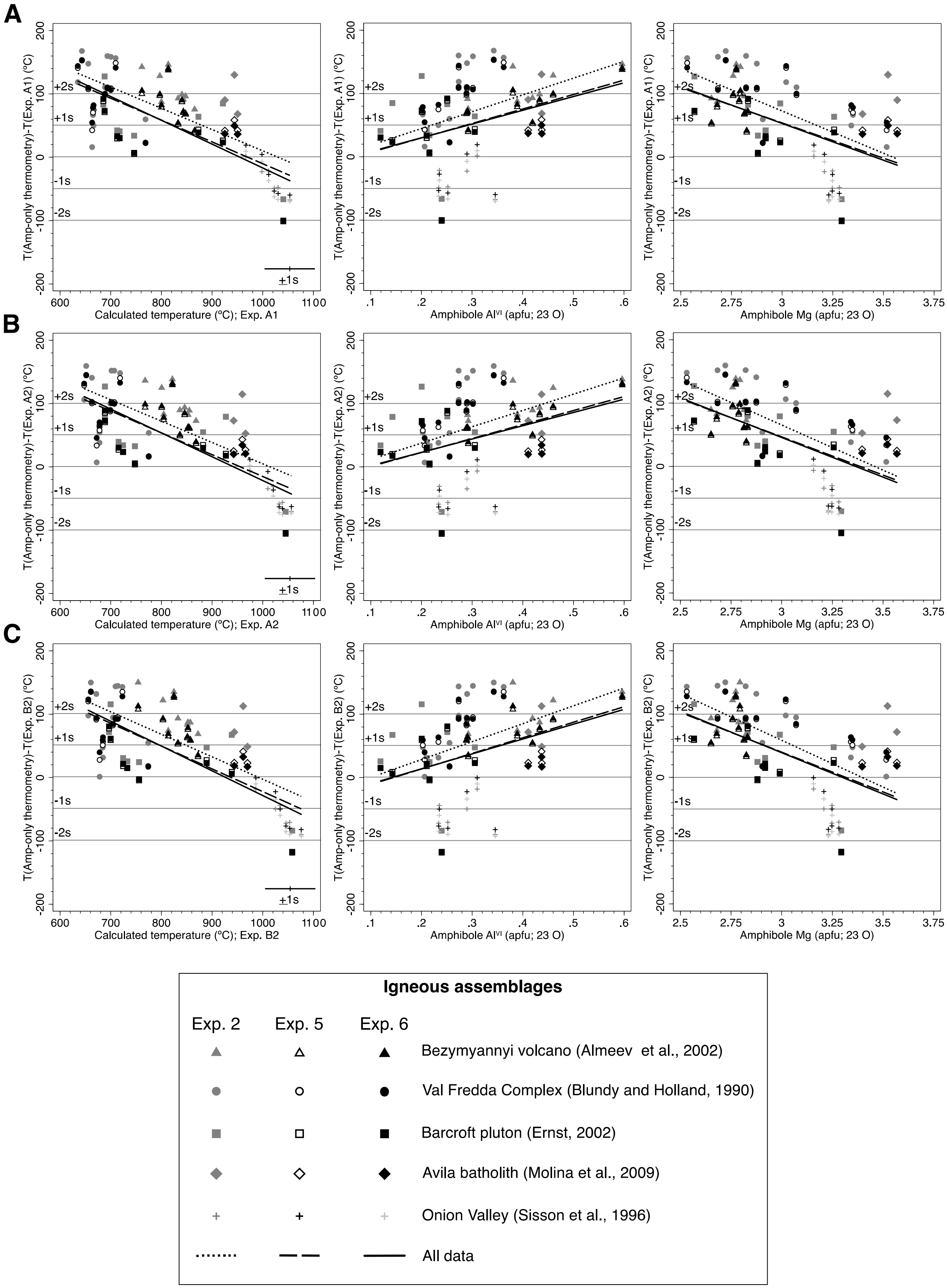

818